

Advanced printing and deposition methodologies for the fabrication of biosensors and biodevices

Laura Gonzalez-Macia, Aoife Morrin, Malcolm R. Smyth and Anthony J. Killard

Received 18th August 2009, Accepted 9th December 2009

First published as an Advance Article on the web 8th January 2010

DOI: 10.1039/b916888e

Advanced printing and deposition methodologies are revolutionising the way biological molecules are deposited and leading to changes in the mass production of biosensors and biodevices. This revolution is being delivered principally through adaptations of printing technologies to device fabrication, increasing throughputs, decreasing feature sizes and driving production costs downwards. This review looks at several of the most relevant deposition and patterning methodologies that are emerging, either for their high production yield, their ability to reach micro- and nano-dimensions, or both. We look at inkjet, screen, microcontact, gravure and flexographic printing as well as lithographies such as scanning probe, photo- and e-beam lithographies and laser printing. We also take a look at the emerging technique of plasma modification and assess the usefulness of these for the deposition of biomolecules and other materials associated with biodevice fabrication.

1. Introduction

The fabrication of biosensors and other related biomedical devices requires the localised interaction of biological molecules and biomaterials with an analyte contained in a sample fluid. This necessitates the placing of the biomolecule in a defined location in the biosensor device. In the past, sensors and biosensors were relatively complex devices in terms of the diversity of parts and techniques required to assemble them. This led to high device manufacturing costs. In recent years, the production of biosensors has moved to fabrication and production processes that allow for high throughput, highly parallel, mass manufacture. Such processes have had the common feature of a system of production based on a flexible, planar manufacturing platform inspired by the traditional print media industry. Indeed, this move towards flexible, planar production is

occurring in the electronics field where traditional silicon-based semiconductor electronics are being replaced with organic and hybrid printed, flexible electronic fabrication methodologies. Such techniques are resulting in the gradual convergence of electronic device production and biomedical device fabrication.

A number of techniques now exist for the fabrication of biosensors and biodevices which allow the highly controlled deposition and patterning of biological molecules and other functionally related materials. As this suggests, two processes must take place; the transfer of the material from a source to the substrate and the precise defined localisation of the material on the substrate. These processes of deposition and patterning are qualities of all advanced fabrication technologies. Some techniques such as inkjet printing, screen printing, microcontact printing, probe-based deposition, gravure and flexographic printing combine deposition and patterning in a single process. Other techniques such as lithography and the newly emerging area of plasma-modification based techniques first bring about surface patterning which subsequently leads to localised deposition.

National Centre for Sensor Research, School of Chemical Sciences, Dublin City University, Dublin, 9, Ireland



Laura Gonzalez-Macia

Ms Laura Gonzalez-Macia is a postgraduate student in the School of Chemical Sciences, National Centre for Sensor Research at Dublin City University where she is undertaking a PhD in the development of biosensors using inkjet printing technologies. She received her MSc in Chemical Sciences from the University of Seville in 2007.



Aoife Morrin

Dr Aoife Morrin obtained her BSc in Chemistry and Mathematics from the Dublin Institute of Technology and a PhD in Chemistry from Dublin City University in Chemistry in 2003. She is currently a lecturer in the School of Chemical Sciences, Dublin City University.

The two key drivers for the suitability and selection of these techniques are the simple, high throughput, low cost mass production capability and/or the creation of smaller feature sizes down to nanodimensions to reduce device size, increase data density, reduce biomaterial requirements and improve device behaviour. The techniques that will see widespread use in the future will be those that can achieve both these requirements.

In this review, we take a detailed look at the range of deposition and patterning methodologies and investigate their application to biosensor fabrication looking at how they are used to deposit biomolecules and other related materials.

2. Inkjet printing

With the increasing ambition to commercialise low cost electronic biosensor platforms, inkjet printing has become one of the most promising techniques capable of manufacturing such devices. In terms of patterning, inkjet printing is one of the most versatile methods available for prototyping. It also allows the deposition of very small volumes of ink (picolitres) in a rapid procedure, achieving high pattern precision and resolution with greater reproducibility than that of other techniques such as screen-printing.¹ Moreover, the fact that no mask is required to pattern the ink and the absence of physical contact between printhead and printed substrate further facilitate the lithographic process.

2.1. Instrumentation

Inkjet printing operates by the highly controlled ejection of low volumes of ink from a printhead employing single nozzle or a series of nozzles. It permits the deposition of tiny droplets (≥ 1 pl) onto a substrate (glass, plastic, metal, *etc.*) with high precision and reproducibility. The resolution of an inkjet printer will depend on the number of nozzles in the printhead. For example, desktop printers have been modified to print functional materials by several research groups. The Olivetti IJP used by Setti *et al.* (2005)¹ to deposit enzymes had 208 nozzles, whereas the Epson Stylus C45 used by Ngamna *et al.* (2007)² possessed just 45 or 48 nozzles, depending on whether black or three-colour printheads were employed. Resolutions higher than 1200 dpi can be reached

with the modified desktop Olivetti system, which means a dot diameter of approx. 15–40 μm , depending on printing material and substrate.¹ There are now several specialised printing systems suited for commercial manufacture on the market. They have been traditionally used as industrial tools for the fabrication of labels, packaging, textile and electronic devices. However, they are latterly being applied in the research field to improve the creation of bioscience devices. Some highlighted characteristics of these systems are shown in Table 1.

Recent work has reported the fabrication of up to 1 μm features by sub-femtolitre inkjet printing of Ag nanoparticles onto an organic semi-conductor-modified surface during the manufacture of organic thin-film transistors (TFTs). In this case, the home made nozzle was manufactured from a very fine capillary glass tube with a tip diameter < 1 μm . The inkjet system was mounted on a three-axis pulse motor stage and both the stage and the head were controlled by computer. Such a feature size permitted the fabrication of high-performance p- and n-channel transistors as well as low-power complementary circuits because the organic solvent in the ink evaporated before hitting the substrate, and so did not harm the organic semiconductor films.

Moreover, improved electric parameters, such as off-state currents, operating voltages and drain current saturation were achieved without any pre-patterning photolithographic process.^{4,5} This achievement could also be applied in the fabrication of the minute electrical interconnections in sensing devices.

2.2. Inkjet printing techniques and mechanisms

Four techniques exist to bring about ejection of droplets from a printhead. These are thermal, piezoelectric, electrostatic and acoustic. However, the most common inkjet printers are based on either drop-on-demand thermal and piezoelectric printheads. Thermal printheads possess a resistor element inside each nozzle (Fig. 1A). When this resistor is heated, ink in proximity to it reaches the threshold temperature, T_i , and a vapour bubble is formed. Usually, bubble formation occurs in just 2 μs , at a temperature of approx. 300 °C. As the bubble grows, the pressure inside the nozzle increases until a droplet of ink is



Malcolm R. Smyth

Prof. Malcolm R. Smyth BSc (1972), PhD in Analytical Chemistry (1976) and DSc (1992). Appointed Professor of Chemistry in 1992 and Dean of the Faculty of Science & Health in 1995. He is a Fellow of both the Royal Society of Chemistry and the Institute of Chemistry of Ireland. Received the Royal Society of Chemistry (RSC) Award in Chemical Analysis and Instrumentation for 1995, and the SAC Gold Medal for

Analytical Chemistry in 1999 from the Analytical Division of the RSC.



Anthony J. Killard

Dr Tony Killard BA (Mod) Trinity College Dublin (1993) and PhD in Biotechnology at Dublin City University (1998). Currently Principal Investigator at the Biomedical Diagnostics Institute and National Centre for Sensor Research, Dublin City University.

Table 1 Characteristics of commercially available research/production inkjet printing systems

Manufacturer/ Model	Type	Material	No. nozzles	Volume drop/pl	Resolution/ dpi ^a	Drop velocity/ $m \times s^{-1}$	Lab/ Industry application	Other characteristics
Pixdro/PL128 Xaar/1001	Printhead Printhead	Glass/silicon —	128 1000	12–30 6	50 360	5–10 6	Industry/Research Industry	Resist pH 1 to 13 TF Technology™ promote the movement of fluid through the printhead and decreasing nozzle blockage
Microdrop/ MD-K-130	Dispenser head	Glass/PTFE	1	20–180	—	2	Industry/Research	Available application- optimized dispenser heads
Dimatix Fujifilm/ DMP-2831 ³	Printing system	Epoxy/Silicon	16	1–10	100 (5080 max.)	—	Industry/Research	Platen heats to 60 °C. User-fillable cartridge
Scienion Flexarrayer S100	Printing system	Borosilicate glass	1–12	100–500	—	—	Industry/Research	Specialized in biological samples (DNA, peptides, proteins and cell arrays)

^a dpi (dots-per-inch).

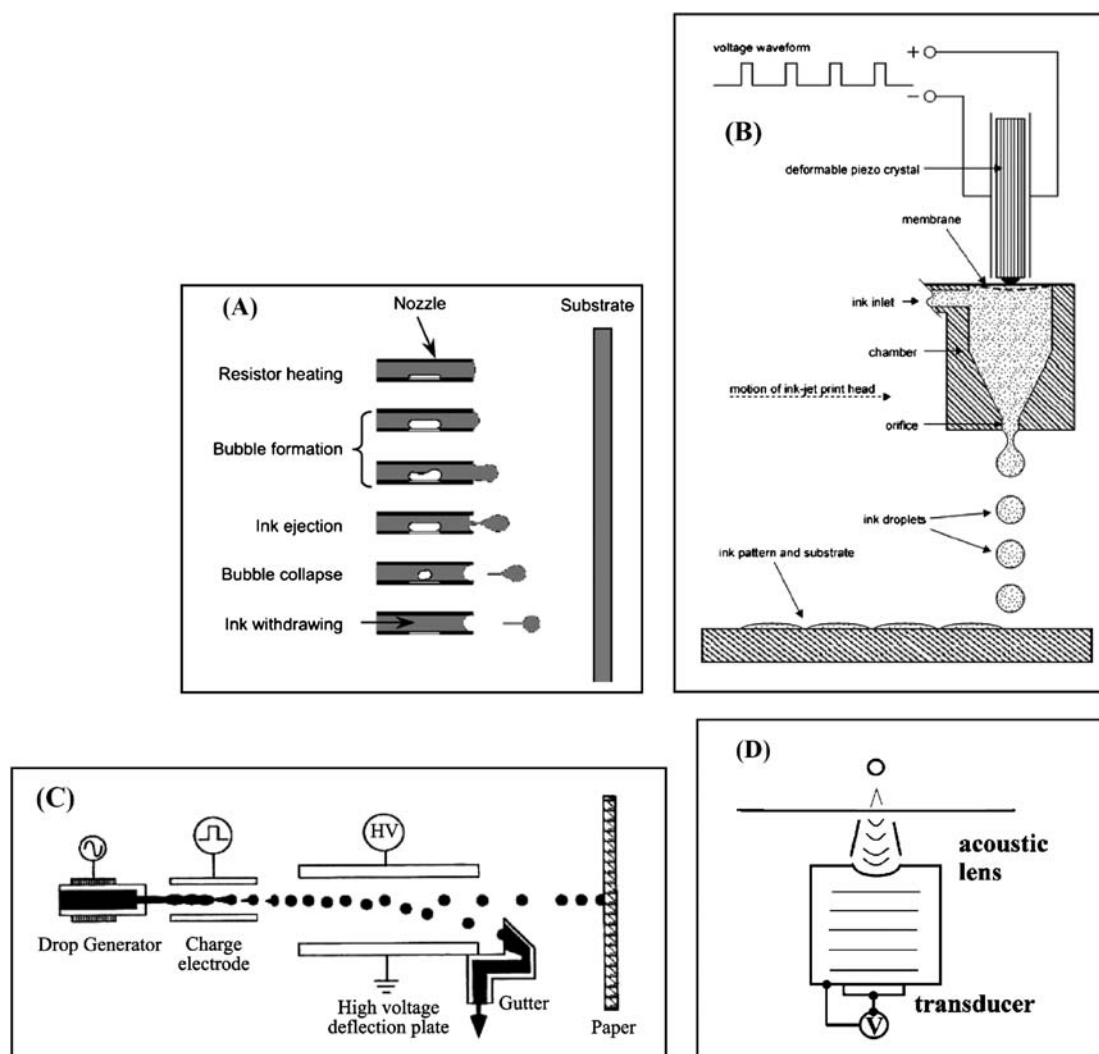


Fig. 1 Principles of operation of inkjet printing ejection mechanisms: (A) Thermal inkjet printing,⁸ (B) piezoelectric inkjet printing,⁹ (C) electrostatic inkjet printing,¹⁰ (D) acoustic inkjet printing.¹¹

ejected through the orifice, almost simultaneously with the collapse of the bubble. The pressure then decreases within the system and the nozzle becomes refilled with ink.^{1,6,7}

The second type of printhead uses a piezoelectric crystalline material confined within the nozzle (Fig. 1B). The application of an electrical field across the piezoelectric material causes its expansion and hence the space available to the ink is reduced, thus increasing pressure and causing the ejection of a drop through the orifice.^{2,7}

Piezoelectric inkjet technology is favoured over thermal printing in many applications as it does not require the high temperatures required for thermal printing (200–300 °C), which can potentially lead to thermal degradation of the ink, particularly when it contains materials such as organics or biological materials.^{11–13} Setti and co-workers reported the activity loss of enzymes after inkjet printing to be 15% when deposited from an Olivetti I-Jet thermal printhead.⁷ Later, Xu *et al.* demonstrated the feasibility of depositing mammalian cells onto agar or collagen-coated glass substrates by thermal inkjet printing. Less than 8% of the cells were damaged during the printing process.¹⁴ These results may reflect the very short time the biological inks were exposed to these temperatures (approx. 2 μ s). Nevertheless, it is important to note that the degree of degradation of the ink may still depend significantly on the thermal sensitivity of the material that it contains and this should be assessed for each ink. Interestingly, significant loss of peroxidase enzyme activity was found when this enzyme was inkjet printed using a piezoelectric printhead. Losses of up to 50% were observed and were attributed to the rapid compression rate of the piezoceramic material. However, this loss could be reduced to negligible levels using slower compression rates. The addition of sugars (trehalose and glucose), which formed extensive hydrogen bonding with the enzyme to protect it, also decreased damage to the peroxidase.¹⁵ The thermal inkjet mechanism is simpler in operation than piezoelectric. In addition, more environmentally friendly solvents are permitted and fewer ink additive modifiers are required as thermal technology does not require as much control of ink viscosity and surface tension compared to piezoelectric technology.¹ In fact, thermal inkjet printing requires viscosities of 1–1.5 cPs whereas piezoelectric inkjet printing requires 5–10 cP viscosity values and surface tension higher than 30 dyn cm⁻¹.^{16,17} However, recently, Lonini *et al.* showed that a biological ink used in a thermal printing system had to be modified in order to avoid nozzle clogging during the printing process. Two commercial inkjet printers, a thermal HP Deskjet 5740 and a piezoelectric Epson Stylus C46, were used for the deposition of an enzyme conjugate solution. An ELISA assay was carried out to assess the activity of the biomolecules after ejection. They reported that the piezoelectric system enabled deposition of biological materials without significant damage. Moreover, while this system did not show any problem of nozzle clogging, the thermal printhead was not able to continuously expel the conjugated solution.¹⁸ It was concluded that surface tension adjustment would be required for thermal inkjet printing, in contrast to earlier reports.^{19–21}

Although the resolutions achievable by thermal and piezoelectric devices are similar nowadays and large improvements have been made with regard to the thermal stability of inks, most of the inkjet printers on the market for research and development

are based on piezoelectric technology. This is primarily driven by the fact that it is a more cost-effective and easy-to-use deposition technology as well as remaining concerns as to the effect of high temperatures on ink constituents.

Although piezo and thermal are the most common mechanisms upon which inkjet printing is based, there are several other drop ejection principles, such as electrostatic- or acoustic-inkjet printing. In electrostatic inkjet printing, a stream of droplets passing between two charged plates is directed into a pattern by varying the electrical potential applied to the plates (Fig. 1C).⁷ Acoustic inkjet printing uses a high-frequency transducer attached to the back of an acoustic lens, which launches an acoustic wave through the lens (Fig. 1D). The lens focuses the acoustic energy, forming a pressure wave that overcomes the surface tension of the liquid just above the lens and expels a drop from the surface.¹¹ Advantages of the electrostatic mode over piezoelectric or thermal modes are its ability to eject fine droplets and the sheer simplicity of the printhead. Electrostatic printing is based on protruding structures of ink formed through an orifice induced by the application of an electric field. These structures form a meniscus and can separate from the tip as fine droplets much smaller than the orifice diameter. In contrast, for example piezoelectric actuators cannot dispense droplets smaller than the nozzle size.²² However, a prerequisite is that the material to be printed is conductive, which limits the range of applications of electrostatic inkjet printing. In 1992, Newman *et al.* developed an amperometric glucose sensor in which both the enzyme glucose oxidase and the mediator tetrathiafulvalene were deposited by electrostatic inkjet printing. Tetrabutylammonium perchlorate was added to the mediator solution in order to increase its conductivity, as the conductivity-based level detector on the inkjet printer was not able to detect the presence of the non-conducting mediator solution alone. A high level of reproducibility and wide operating range were achieved with these electrodes compared to those developed with other techniques at that time.¹² A conductive mixture of D₂O, sodium dodecyl sulfate (SDS) and micelle-suspended single wall carbon nanotube (CNT) (5% w/v) solution has been recently deposited using electrostatic inkjet printing. The applied voltage was kept at 2.5 kV, which resulted in 10 μ m-diameter droplet formation.²² The deposition of CNTs has also been reported by means of a home-built electrostatic printhead whose nozzles housed a needle inside a capillary to eject droplets when an electric pulse voltage was applied to it. The surface tension of the liquid to be ejected was found to be a critical parameter for the printing process, and was regulated by adding ethanol to the CNT/water ink. The resolution obtained was approx. 45 μ m, although this parameter varied with the applied voltage.²³

Organic thin-film transistors have been fabricated by the printing of soluble polymeric organic semiconductors (derived from polythiophene) using acoustic inkjet printing. These polymeric semiconductors, dissolved in organic solvent, were printed at a resolution of 35 μ m, and yielded a uniform film deposition on hydrophobic gate dielectrics in a single processing step, which is difficult to obtain by other deposition techniques such as spin-coating.²⁴ The performance characteristics of these transistors were comparable to those of devices prepared by spin-coating, but the volume of ink required was lower and hence less waste was generated. The absence of nozzles in the acoustic inkjet

printer overcomes the problem of nozzle clogging, a common issue in thermal and piezoelectric inkjet printers. Nevertheless, the single ejector printhead has not reached the success of the thermal or piezo to date, possibly because it does not have a precedent in the conventional desktop printer.

2.3. Ink materials

To develop an ink that is printable, rheological properties such as viscosity and surface tension are critical. As a droplet is expelled from the orifice of a nozzle, energy goes into viscous flow, surface tension of the drop and kinetic energy. The viscosity must be low enough to allow the channel to be refilled in about 100 μs .²⁵ The surface tension must be high enough, and the pressure low enough, to hold the ink in the nozzle without dripping. The viscosity of the ink should be in the range of 3–20 cP and the surface tension between 20 and 70 dyn cm^{-1} to avoid clogging or dripping and to ensure continuous film formation onto the substrate surface in a piezoelectric inkjet printing system.^{2,17} These precise characteristics depend on the ejection mechanism and the end-application for the printed films.^{22,23} It is often necessary to add wetting agents, pigments and polymeric compounds to improve resolution and printed film quality. For example, surfactant Tween 80 was added to an aqueous poly(3,4-ethylenedioxythiophene)/polystyrene sulfonic acid (PEDOT/PSS) dispersion to obtain the necessary surface tension for printing using a thermal printer.¹ Different concentration ratios of ammonium peroxydisulfate (APS), dodecylbenzenesulfonic acid (DBSA) and aniline were investigated by Ngamna *et al.* to obtain polyaniline (PANI) nanoparticle dispersions with suitable particle size and viscosity to be inkjet printed with a piezoelectric printer. They observed that excessively high levels of the DBSA

surfactant increased the resistivity of the polyaniline dispersion. Whereas maximizing the amount of APS achieved higher conductivities of the material, but the resulting particle size was too large, rendering it unfeasible for inkjet deposition. Therefore, a compromise between the three starting materials for polyaniline nanoparticles synthesis was found to enable printing of the nanoparticles as well as maintaining good conductivity.² Van den Berg *et al.* used poly(vinyl methyl ether)-block poly(vinyl-4-butyric acid) diblock copolymer as a colloidal stabilizer for TiO_2 particles in an aqueous ink. The ink viscosity could be controlled by increasing the temperature above 37 $^\circ\text{C}$ (the critical flocculation temperature). Changes in temperature altered the colloidal stability of the particles in the ink and caused gelation of the ink. This property was exploited to limit material transport during drying and to eliminate the “coffee ring” effect – deposits left by evaporating drops – in printed features.²⁶ Recently, Soltman and co-workers have also reported how controlling substrate temperature could eliminate the coffee ring effect. A heated poly(4-vinylphenol)-coated glass substrate showed an enhanced coffee ring compared to room temperature drying due to greater evaporation at the drop edge when a PEDOT/PSS ink was deposited by piezoelectric inkjet printing. Analogously, a cooled substrate suppressed edge evaporation and eliminated the coffee ring at the feature’s edge, as is shown in Fig. 2.²⁷

The range of functional ink materials that can be printed has increased greatly during the last number of years. Inks can be printed directly to an unmodified substrate or after a pre-treatment in order to induce air-stability and solution processability. For example, PEDOT can be doped with PSS to permit its dispersion in water to obtain a printable ink.^{8,28–30} Resulting polymer films possess good conductivities (1–10 S cm^{-1})²⁹ and high stability in the solid film form and have been used as

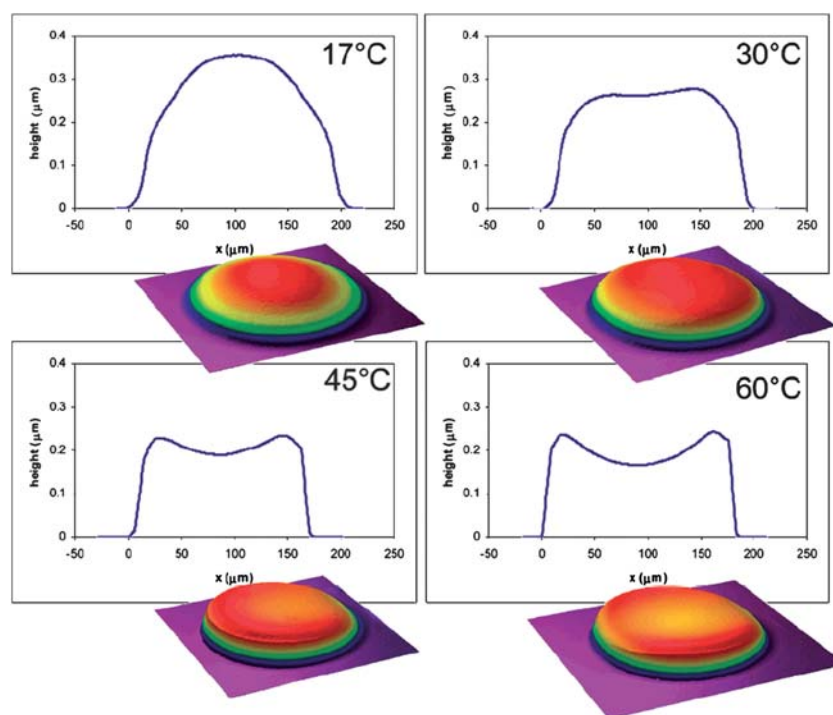


Fig. 2 Cross section and 3D projection from an optical profilometer of single drops printed at the given temperature.²⁷

a platform for glucose oxidase (GOD) deposition for biosensor fabrication¹ and for the source–drain and gate electrodes in the fabrication of thin film transistors²⁸ and other electronic circuits.³⁰ Surfactant-dispersed PANI nanoparticles have been inkjet printed using a piezoelectric device by Morrin *et al.* Conducting polymers such as PANI are important promising materials in terms of both optical and electrochemical sensing and are being extensively researched at a nanostructured level, where processability can be significantly improved. Several methods such as spin-coating,^{31,32} self-assembly^{33,34} and screen-printing^{35,36} have been used to pattern them. Inkjet printing of conducting polymer nanodispersions has been most recently achieved.² This breakthrough in their processability is very important for looking towards commercial sensor applications.³⁷ Gold and silver colloidal nanoparticles⁹ have been inkjet printed and subsequently sintered at 300 °C to form a deposited material structurally and morphologically comparable to bulk metal. This method has been used to build 3-D microelectromechanical systems (MEMS) and electrical circuitry, offering a potentially more cost-effective fabrication approach in comparison to techniques such as lithography or molten-metal droplet deposition as cost and fabrication time is decreased significantly. In addition, employing a nanoparticle colloid ink instead of molten

metal avoided metallic oxidation and printhead clogging issues. In another approach, Smith *et al.* fabricated circuits by inkjet printing a silver-based organometallic solution that was then reduced to metallic silver by heating the printed tracks to 150 °C. This low temperature curing process compared to that used conventionally permits the deposition on to a much wider range of flexible, polymeric substrates.³⁸

Water-insoluble organic materials have been inkjet printed by means of the formation of stable oil-in-water microemulsions. Inside the droplets of the microemulsion, the functional organic molecules are dissolved in a volatile water-insoluble solvent, such as toluene. After printing, the droplets rapidly evaporate to form an ordered structure of organic molecules on the substrate surface. Different organic nanoparticle cluster sizes can be formed on the surface depending on the evaporation time required for the organic solvents used and the percentage of these solvents in the initial ink as is shown in Fig. 3. Magdassi and co-workers found that the size of the nanoparticles decreased with increasing toluene concentration in an oil-in-water microemulsion, from approx. 300 nm for microemulsions with 4 wt% toluene to 55 nm for 30 wt% toluene ink.¹³ This method can be applied to a large variety of molecules, including polymers, for applications such as organic light-emitting diodes, eliminating

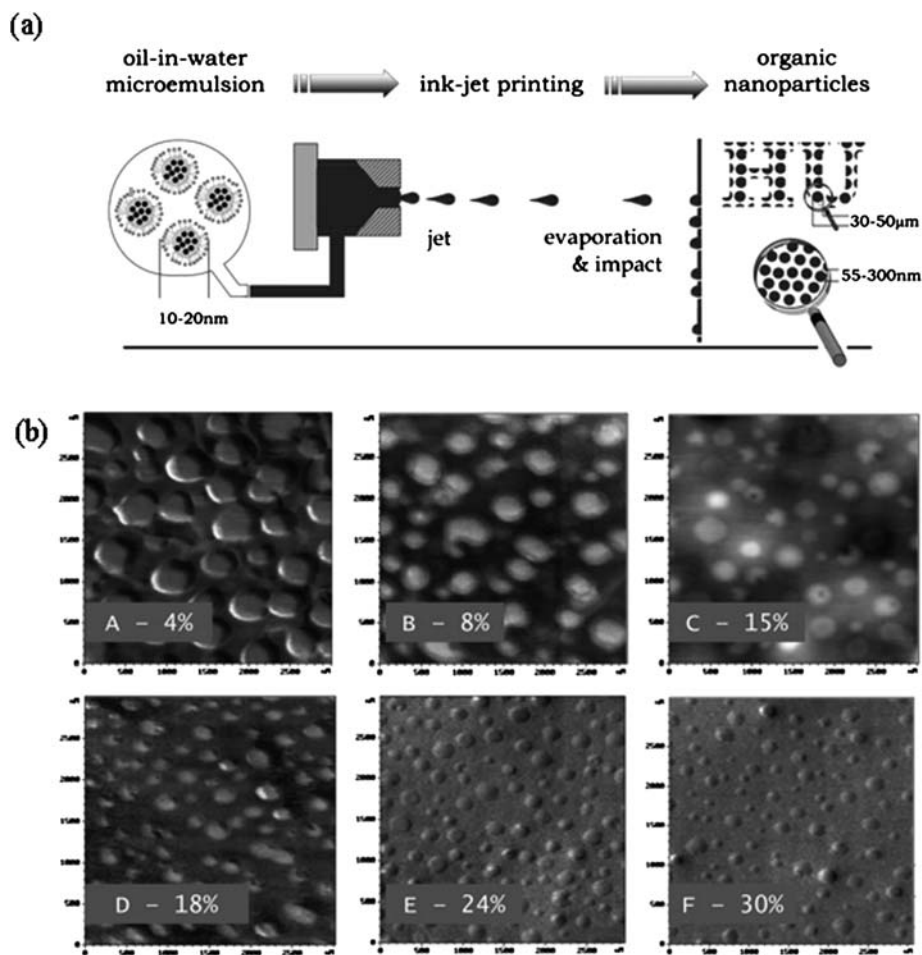


Fig. 3 (a). Schematic presentation of microemulsion conversion into nanoparticles by ink-jet printing. (b). AFM images of the organic nanoparticles formed after inkjet printing the microemulsion ink. A decrease in the nanoparticle size with increasing initial toluene concentration is observed.¹³

the need of previous ink processing. However, thermal printing is not compatible with this technique because the high temperature required for bubble formation in the printhead would induce rapid evaporation of the organic solvents, preventing the formation of droplets and damaging the material.

2.4. Applications

Most large scale applications for inkjet printing carried out to date have been based on high value products such as solar panels, OLED displays, electronic components, graphics, packaging and other industrial marking. However, many are now turning to its application in biosensing devices, for both industrial and R&D purposes. Thus, as well as conducting polymer and organic materials, new biological materials have been developed and printed using this technique.

Hasenbank *et al.* recently developed thiol-modified gold electrodes where the thiols and multiple biotinylated proteins were deposited using a piezoelectric inkjet printer. A mixed thiol solution consisting of polyethylene glycol thiol (PEG) and biotinylated alkyl thiol (BAT) was initially inkjet printed on to Au-modified glass slides. A streptavidin layer was assembled on the patterned BAT layer after the incubation in a streptavidin solution and then two biotinylated proteins (b-horseradish peroxidase and b-BSA) were inkjet printed on the streptavidin surface. Introducing BSA and HRP antibodies and using surface plasmon resonance (SPR) microscopy, these electrodes were found to be highly specific and amenable to multi-analyte sensing as is shown in Fig. 4.³⁹

Many enzymes have been inkjet printed in the past 15 years since Newman and co-workers first deposited GOD using a piezoelectric printer.¹² Roda *et al.* reported the deposition of HRP on cellulose paper by using a desktop thermal printer. A small amount of sodium dodecyl sulfate (SDS) was added to the enzymatic ink in order to obtain a suitable surface tension of 55 dyne cm⁻¹. The diameter of the printed spots was 0.2 mm and the amount of enzyme in each spot was evaluated by means of chemiluminiscent detection.¹⁹ Until now, most printed enzymes have been deposited using piezoelectric inkjet printers as it was thought to affect the activity of the enzyme to a lesser extent. However, Roda *et al.*¹⁹ and later Setti *et al.*¹⁷ showed that enzymes could be deposited by a thermal printer with no significant differences in the enzyme activity. β -Galactosidase and GOD were printed and their activity was checked by spectrophotometric assay. A food dye (Brilliant Blue FCF, E133) was

added to the biological ink as a colorimetric probe to visualize the printed area and determine the volume of ejected ink (approx. 0.76 $\mu\text{l cm}^{-2}$). Other components of the biological ink included EDTA as an anti-microbial agent and glycerol as stabilizer and viscosity regulator. Inkjet printed GOD was used in the fabrication of an electrochemical glucose biosensor prototype and it showed responses to glucose when the enzyme was deposited directly onto the substrate, and in the presence of ferrocenemethanol (FeMeOH) as a mediator.

Single-stranded DNA (ssDNA) oligomers were printed using a commercially available piezoelectric system. The printer device (Microdrop, MD-P-705-L) consisted of a three-axis micro-positioning system and piezo-driven autopipettes (Microdrop, AD-K-501) with 70 μm nozzle diameters which enabled a droplet volume of 180 pl. First, alkanethiols were deposited on selected Au-coated cantilevers to prove the feasibility of the system at delivering different materials simultaneously. Then, ssDNA previously modified with a thiol linker was deposited using the same mechanism and its functionality was verified in a sensor setup using an appropriate complementary target.⁴⁰ Earlier, Okamoto *et al.* printed DNA onto a glass substrate by means of a thermal system. 5'-terminal-thiolated oligonucleotides and a heterobifunctional crosslinker were used to attach DNA covalently to the surface. To decrease the shearing stress of the material, glycerine, urea and thiodiglycol were added as wetting agents and acetylenol to reduce the viscosity. Eight-by-eight spot microarrays of oligonucleotides were printed and evaluated by hybridizing to tetramethylrhodamine-labeled target oligonucleotides containing a base sequence complementary to the probe sequence. Damaged DNA strands were not observed in the fabricated microarrays despite the thermal ejection process. The system was successfully applied to identify mutations of the p53 gene from two cell lines of human oral squamous cell carcinoma.²¹ A biochip for the detection of human fragile histidine triad (FHIT) – a tumour suppressor gene – was also fabricated by printing techniques. Microspots of PCR-amplified genomic DNA extracts from mice tumours were deposited by thermal printing forming a 4 \times 4 matrix on the substrate, which was a Zetaprobe membrane. In this case, ethanol was added to the biological ink to reduce the viscosity and surface tension and to facilitate wetting of the ejection capillaries.²⁰

Another important area for inkjet printing in biomedical applications has focused on printing cells in order to study how they interact and perhaps even to fabricate organs for implants. Recently, human cells were deposited from a suspension of the

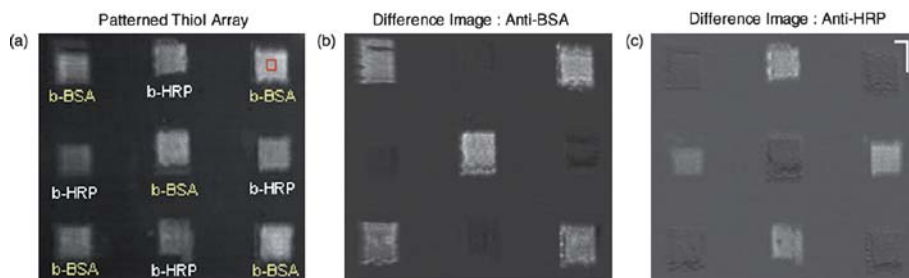


Fig. 4 Multi-analyte protein patterning using the BAT/PEG and streptavidin linker system. (a). SPR image of a 3 \times 3 patterned BAT/PEG array with streptavidin and biotinylated BSA or HRP layers, as indicated. A PEG thiol layer surrounds the patterned protein layer; (b). Change in SPR signal after exposure to an anti-BSA antibody; (c). Change in SPR signal after exposure to an anti-HRP antibody.³⁹

HT 1080 fibrosarcoma-derived cell line using piezoelectric printing. No adverse effect on cell viability after printing was observed compared to the behaviour of control samples. Moreover, it was reported that the amplitude of the pulse had a small influence on cell survivability (from 98% with a 40 V pulse to 94% with an 80 V pulse). However, the stability of cell suspensions in the printer reservoir showed significant reductions in printing efficiency after 20 min due to the formation of some cell agglomeration or sedimentation.⁴¹ Although some successful attempts with hamster¹⁴ and human cells^{41,42} have been carried out so far, there is a long way to go and several challenges to overcome to make the use of inkjet printers viable for cell patterning.⁴³

An extremely powerful capability of inkjet printing technology is that it can facilitate multi-analyte co-patterning, as has been shown for DNA printing.^{20,21,40} The printing systems possess multiple printheads or micropipettes, depending on whether they receive ink from a reservoir (dispense mode) or by fluid aspiration (pipette mode). When polymeric inks are multi-patterned, three different protocols can be followed depending on if the inks are mixed before, during or after inkjet printing. If the inks are mixed before printing, new solubility and viscosity characteristics are required from the “just-created” ink, which means an added drawback to the printing process and makes this option less attractive. On the other hand, mixing during the printing process requires a single printer, but with a separated mixing chamber. The high kinetic energy from the impacting droplet seems to ensure perfect ink mixing, which makes the mixing on the substrate method the simplest option for the multi-patterning process. However, further studies should be carried out to optimise the homogeneity and volatility conditions.¹⁷ Hwang *et al.* used a colour inkjet printer cartridge where each of the three compartments (red, yellow and blue) was filled with different solutions used as catalyst precursors for carbon nanotube (CNT) synthesis. By means of the built-in software, the volume ratio of different inks was easily controlled, facilitating the study of the optimised proportions in the synthesis.⁴⁴

Although inkjet printing technology has been exploited for the last number of years for the printing of functional materials, new applications, especially in the biosensing field, are constantly emerging. These printing techniques are attracting a lot of interest for material patterning, not only due to the highly controlled amount of ink that can be directed onto the substrate, but also because of the absence of direct contact between the print head and the substrate, making it particularly suitable for use on contact-sensitive substrates, such as membranes.⁸ Its unique characteristics, range of materials that can be printed, non-contact mode and its simple handling make this technique feasible to large-scale production. In addition, inkjet printing permits the use of environmentally friendly solvents and the waste production is minimal as small quantities of printed material are required, as opposed to more traditional deposition techniques such as screen-printing. The wide range of publications on sophisticated biosensing applications for this technique shows the need of adapting the technology in order to make this technique become a mass production process in biosensor manufacture.

In short, the range of materials amenable to printing has risen greatly during the last decade, permitting the deposition of

delicate biomolecules such as enzymes, DNA and even cells without damaging their activity. By adding modifying agents to the ink, the viscosity and wettability required for the printing process can be achieved. Inkjet printing has proven to be a useful technique to pattern a high variety of material simply and quickly; key characteristics for the application of any deposition technique.

3. Screen-printing

One of the most widely used techniques in the manufacture of disposable biosensors to date has been screen-printing. This method has been widely reviewed since it is a conventional technique for film deposition^{45,46} and patterning of both organic and inorganic materials,¹¹ so only improvements recently achieved will be reported here.

During the screen-printing process, a liquid paste is forced through a mesh screen mask by a rubber *squeegee*⁴⁷ in order to form a pattern onto the substrate surface, as is shown in Fig. 5. The screen is a negative of the required image, and a great range of patterns can be managed by using different commercially available masks.⁷ The imaged pattern on the screen will possess a mesh with defined thickness that will allow a quantity of ink through when the squeegee is applied. Generally, the conductive inks used for screen-printing are comprised of three basic constituents: a powdered metallic (gold, platinum, silver) or non-metallic (graphite) conductor, a binding agent (glass powder, resins or cellulose acetate) and a solvent (terpineol, 2-ethoxyethanol, cyclohexanone, ethylene glycol). Non-conductive, insulator or adhesive inks are also printed by means of this method. The solvent provides the suitable viscosity for the printing process and volatility for thermal curing, whereas the

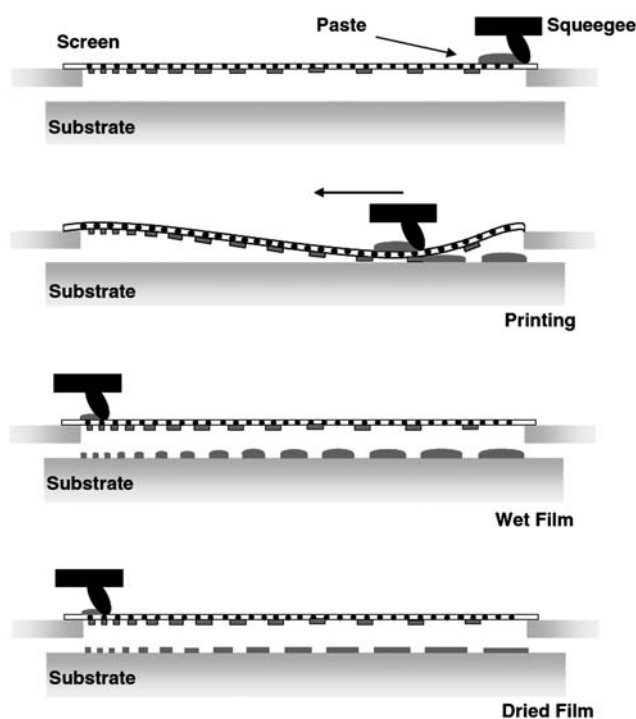


Fig. 5 Schematic diagram of the screen-printing process.⁵⁰

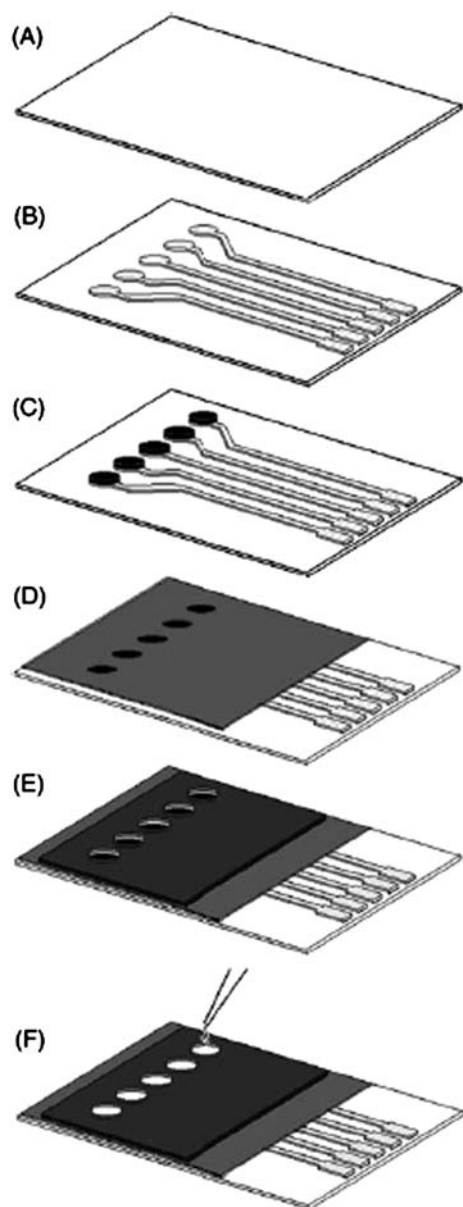


Fig. 6 Schematic diagram of the fabrication process for all-solid state planar-type sensor array: (A) polycarbonate substrate (50 × 75 mm), (B) silver ink printing, (C) graphite ink printing, (D) insulator layer printing, (E) cavities for the sensors, and (F) deposition of different PVC membranes.⁴⁹

binding agent improves the mechanical strength of the ink and its adhesion on the substrate.^{46,48} Once printed, the freshly deposited material is cured by heat^{48,49} or UV irradiation.^{47,48}

Traditionally, screen-printing has been used as a tool to pattern substrates which would be subsequently used for the fabrication of biosensors. Screen printers tend to be used for the manufacture of the electrode materials and the biological molecule is dispensed in some other way.^{47,51–54} However, Lifescan (Milpitas, CA) produce their glucose sensor using an enzyme ink deposited by screen-printing. Recently, a tiny glucose sensor chip with a blood sample volume as small as 200 nl was created. The carbon paste ink was printed on a PET substrate first, and the insulation and adhesive layers were deposited on top by screen-

printing. However, the enzyme (GOx) and the mediator (potassium ferricyanide) were deposited by drop-coating. The improvement of this system was based on the screen-printed adhesive layer. Conventionally, an adhesive layer was placed to form the inner walls of the chip cavity with a thickness of approx. 100–300 μm. However, thicknesses of less than 50 μm were reached by screen-printing the adhesive ink, thus reducing the blood sample volume required for the analysis.⁴⁷ A tyrosinase (Tyr) biosensor for the determination of carbamates and organophosphorus pesticides has also been developed. A cobalt (II) phthalocyanine (CoPc) modified cellulose-graphite composite was screen-printed onto a polycarbonate substrate and the enzyme was immobilized by cross-linking with glutaraldehyde and bovine serum albumin. The biosensor was optimized utilizing catechol as substrate and investigating the inhibitory effects of some organophosphorous (methyl parathion and diazinon) and carbamates (carbaryl and carbofuran) on the Tyr biosensor response.² Karadeniz *et al.* used commercially available graphite screen-printed electrodes modified with multi-walled carbon nanotubes (MWCNT) as a platform for the deposition of DNA. Specific sequences of Hepatitis B virus (HBV) DNA were dispensed by drop-coating. DNA hybridization was monitored electrochemically by measuring the guanine signal observed during the process.⁵⁵

Some approaches to screen-printing biological inks have been attempted as this would potentially increase the homogeneity and simplicity of the sensor fabrication process. However, the rheological requirements of the screen-printing inks make this less straightforward. Moreover, the extreme conditions often required for curing after screen-printing (high temperature or UV cure) could easily damage the activity of the biological compounds. Having said this, commercial glucose biosensors are successfully produced using enzymes in screen printing inks such as the OneTouch® test strips from LifeScan, Inc. Wang *et al.* have prepared electrochemical biosensors by screen-printing carbon-based inks containing rabbit immunoglobulin G⁵⁶ or GOx.⁵⁷ The immunosensor was fabricated by adding graphite powder and rabbit IgG to a previously prepared sol-gel solution, which facilitated the cure of the ink at 4 °C after printing. A relatively fast and highly sensitive response comparable to other electrochemical immunosensors and ELISA assays was achieved with this printed device. For the glucose sensor, a carbon paste ink containing copper hexacyanoferrate and GOx was screen-printed onto an alumina ceramic plate and cured at 60 °C. The presence of the catalyst in the ink decreased the potential for the reduction of the enzymatically-generated H₂O₂ a region where interferent reactions were negligible, simplifying the sensor fabrication. The optimization of a glucose biosensor fabrication methodology has been recently reported by using a single-step screen-printing method. The ink consisted of carbon, CoPc and GOx in a water-based polymeric binder and was printed onto a PVC substrate and left to dry overnight at room temperature. The use of water-based inks as an alternative to the solvent-based inks can facilitate the incorporation of enzymes or other biomolecules into the ink without damage, either from the solvents or possible thermal damage during the cure process.⁵⁸

Several non-biological materials have been deposited using screen-printing for fabricating sensing devices. Gutierrez *et al.* developed a disposable screen-printed sensor for the

simultaneous determination of NH_4^+ , K^+ and Na^+ ions in water samples. Conductive silver and graphite pastes first and epoxy resin later were screen-printed to a polycarbonate substrate generating the five-sensor arrays. Finally, the ion-selective PVC membrane, which contained the recognition elements (ionophores) for the ions, was manually deposited as is shown in Fig. 6. The potentiometric electronic tongue created demonstrated good sensitivities for NH_4^+ , K^+ and Na^+ in synthetic waters, whereas Na^+ determination showed some errors in natural surface waters.⁴⁹ Screen-printing has also showed to be an appropriate technique for the deposition of nanostructured materials such as SnO_2 , TiO_2 , In_2O_3 , $\delta\text{-Al}_2\text{O}_3/\text{Cu}_2\text{O}$ or LaFeO_3 . The fabrication of layers with nanosized nanoparticles enhanced the extension of surface exposed for gas adsorption, creating semiconductor-based devices for gas sensing applications (CO , H_2 , NO_2 , CH_4).^{59,60} Other group of materials with sensing applications and suitable to be screen-printed has been conducting polymers. These materials have been widely used because environment-induced changes to the doping level or band structure lead to changes in their electrical properties, which can be easily detected. These changes are reversible, which is a key advantage of their applications, but the response time can be slow due to the need for diffusion of chemical species into the bulk of the polymers.⁶¹ As an example, the electrical conducting polymer polypyrrole (PPy) was deposited by screen-printing during the fabrication of a tin dioxide-based sensor for gas detection. The method was shown to be the simplest one for preparation of a multilayer sensor, providing a device with higher sensitivity to CO_2 gas and better stability than those reported to date.⁶²

In short, screen-printing is still widely used in biosensor manufacture because of its robustness, simplicity, high throughput and low cost for mass production. Although it requires a screen stencil and is a contact method, there is no other technique as rapid and as scaled-up as screen-printing reported to date for mass biosensor fabrication. Its characteristics make it a unique method, which can also be combined with other techniques such as inkjet printing or nanografting to achieve very high resolutions (nm) or to pattern biological compounds on previously screen-printed substrates.

4. Roll-to-roll printing

Traditionally used for printing newspapers and magazines, roll-to-roll printing methods are becoming an interesting choice for the fabrication of flexible devices. Based on inking and stamping

techniques, the roll-to-roll process involves the transfer of the ink from the patterned printing roll on top of a flexible substrate.^{63,64} Gravure printing, flexographic printing and roll-to-roll nanoimprinting are some of the currently used roll-to-roll techniques.

In *gravure printing* the pattern to be printed is engraved into a rotary printing cylinder. During the printing process, the engraved cells are filled with the ink and a flexible doctor blade is used to remove excess ink. Then, the ink on the printing roll is transferred to a substrate when the roll is brought into contact with it, as is shown in Fig. 7. Materials such as conducting polymers^{65–67} and ITO nanoparticle dispersions^{63,67} have already been deposited by gravure printing. Tuomikoski *et al.* printed ITO structures on poly(ethyleneterephthalate) (PET) foils to be used as anodes in polymer light-emitting devices (PLED). These printed components showed no significant differences in the coating properties compared to those obtained by spin-coating and were used as a substrate for the deposition of the conductive polymer PEDOT:PSS, essential in the manufacture of PLED structures.⁶⁷ Typical printing speeds of about 40–60 m/min were applied and line densities of 110 lines/cm and 70 lines/cm were obtained for ITO and PEDOT deposition, respectively. Depending on the solids content in the inks and the geometry of the gravure cells, thicknesses ranging from 0.2 to $>1\ \mu\text{m}$ were realized in a single print step. However, the high pressure required for this process and the low resolutions obtained are drawbacks that have prevented the use of this technique in the manufacture of high-precision devices.

In *flexographic printing*, a uniform film of ink is first applied to the raised portion of the patterned flexography rubber which coats the printing roll. Then, it contacts the substrate and transfers the images onto it. The pressure needed in this technique is lower than that required for gravure printing, and the resolution is also marginally better. Flexographic printing is mainly used for short and medium runs, whereas gravure printing is used for longer processes as the cost of the cylinders makes it expensive for short runs.

Roll-to-roll nanoimprinting is a flexographic technique which allows patterning of submicron features at relatively high speeds (up to 20 m/min). During the process, a flexible Ni-shim is turned on a printing roll as is shown in Fig. 7, and the pattern is then transferred onto the substrate surface using pressure, generally at elevated temperature. Electrical heaters inside the roll or a hot air dryer help to reach temperatures above the glass transition temperature of the polymer during the patterning process. The nickel stamps used as shims are usually fabricated by electron beam lithography and electrotemplating and subsequently

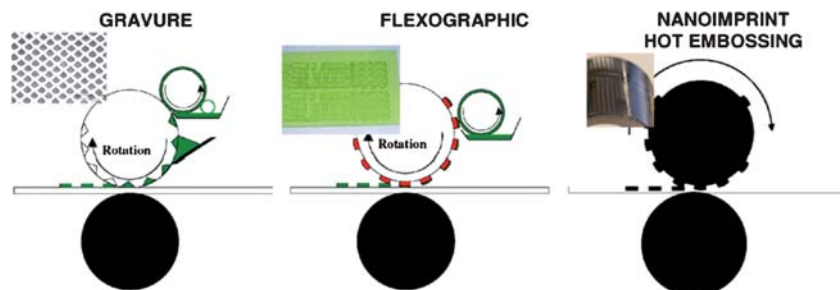


Fig. 7 Schematic process of roll-to-roll gravure, flexographic and nanoimprinting methods.⁶⁶

attached onto the printing cylinder mechanically or by using adhesive double sided tape.^{66,68,69}

Combinations of different roll-to-roll methods have been reported to improve the quality of the pattern. Makela and co-workers carried out gravure printing and nanoimprinting consecutively in a single cycle by means of a custom-made laboratory scale machine. The gravure unit was used to coat 60 μm thick propylene substrate with a layer of the conducting PANI-DBSA polymer, which was subsequently dried by means of an electrical curing element at 180 $^{\circ}\text{C}$. Nanoimprinting was then used to pattern the freshly coated area at 0.2–1.0 m/min speed using 5–14 MPa pressure to remove the polymer. Gratings with 500 nm wide lines imprinted into the conducting polymer film were demonstrated by AFM.⁶⁶ The same group fabricated double-sided-imprinted structures on a cellulose acetate film by a simultaneous roll-to-roll process. A custom-made roll-to-roll imprinting device with two embossing units was used at the same time. The pattern consisted of 1 μm -dot structures with 200–250 nm height on a Ni-stamp, which were stamped on the cellulose substrate by using 8 MPa printing pressure at 105 $^{\circ}\text{C}$ (the Tg of cellulose acetate is 120 $^{\circ}\text{C}$). AFM images showed 159–196 nm height structures on the bottom side and 108–130 nm on the upper one, as is shown in Fig. 8. Although hundreds of meters of cellulose acetate film were printed, no marked degradation of the Ni-stamp was observed.⁶⁹

Roll-to-roll techniques are feasible for large area patterning in the biosensor manufacture field. Several companies already provide many materials for flexographic or gravure printing which can be used for biosensing applications such as blood glucose or immunoassays. Moreover, a large number of patents claim this procedure as a tool for the deposition of the different materials for biosensor fabrication.^{70,71} For example, Shinozuka and co-workers developed a dehydrogenase biosensor to detect analytes such as alcohols, galactose, glucose or cholesterol in the presence of a tetrazonium salt by means of the formation of a formazan product, which was electrochemically detected. They claimed the application of roll-to-roll printing methods for the fabrication of carbon paste electrodes for use as a platform in biosensor manufacture.⁷²

Roll-to-roll techniques offer a method of fabricating large-area electronics and optical structures at low cost. They have also been widely used for the fabrication of biosensors. However, like screen-printing, roll-to-roll has been mainly exploited in the creation of biosensor platforms and, as yet, few examples of

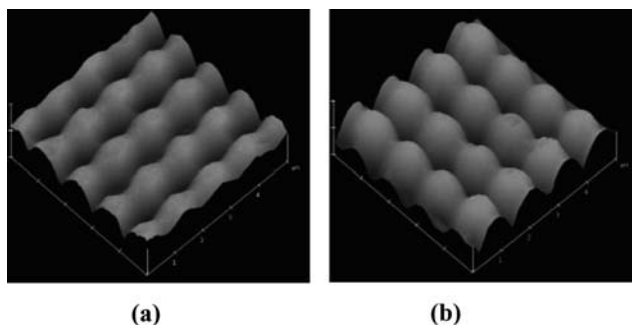


Fig. 8 AFM images of simultaneously imprinted double-sided structures. Upper (a) and bottom (b) sides of the film.⁶⁹

whole biosensor fabrication processes have been reported using this type of technique, possibly due to the low resolutions obtained with most of the roll-to-roll methods.

5. Microcontact printing (μCP)

Microcontact printing is another technique utilized for patterning surfaces at both micrometer and sub-micrometer^{73–76} resolution. It has often been used for depositing proteins^{73,77–79} to suitable surfaces for biosensor fabrication. This technique belongs to the group of techniques known as soft lithographies as it uses stamps or channels fabricated in an elastomeric material for pattern transfer.⁷³ Microcontact printing is used as an alternative to inkjet printing as it is more flexible in terms of the ink rheology requirements as well as having significantly higher resolution than inkjet printing. Indeed, resolutions at the nanometre length scale have been reported.^{78,80}

5.1. Principle

Microcontact printing is based on the selective transfer of the material of interest (alkanethiols, silanes, proteins) from the patterned stamp to a substrate surface. In the first instance, the stamp is fabricated by casting a polymeric elastomer (usually polydimethylsiloxane, PDMS) against a “master” template following the steps shown in Fig. 9a. Masters are generated by photolithography or one commercially available diffraction gratings. Since this method was first described by Whitesides and co-workers for patterning self-assembled monolayers (SAMs) of alkanethiols onto gold substrates, many of the biomolecule patterned using this technique have used alkanethiol-based SAMs on gold.^{73,81,82} However, several studies of direct biomolecule deposition from the elastomeric stamp onto the substrate have since been reported, without the use of alkanethiol-based molecules as a mediator.^{77,83} During the procedure, the stamp is “inked” with a solution of the material of interest (*e.g.* an alkanethiol in ethanol) and brought into contact with the surface, *e.g.* gold. The compound is then transferred to the areas where the stamp contacts the substrate, forming a patterned self-assembled

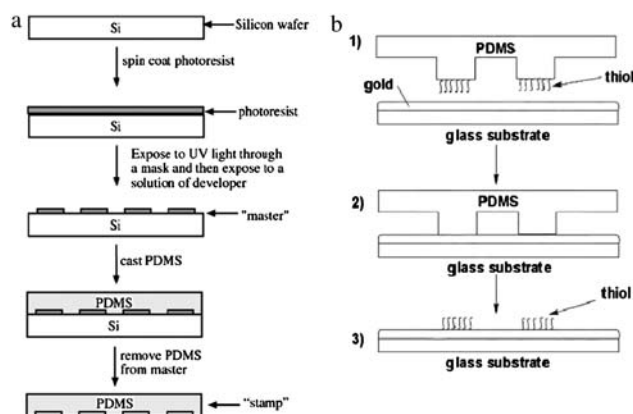
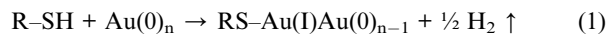


Fig. 9 (a). Scheme of fabrication of a PDMS stamp from a “master” template.⁵⁶ (b). Schematic illustration of a μCP procedure: 1) PDMS stamp with raised regions covered with SAM; 2) PDMS stamp is brought into contact with gold surface to transfer SAM; 3) patterned SAM monolayers.²⁸

monolayer. Fig. 9b shows a typical microcontact printing process.¹¹

SAMs of alkanethiols are highly packed, dense monolayers which form when a clean surface of gold is exposed to a solution (or vapour) of an alkanethiol, according to eqn (1):



The terminal functional group (R) of an ω -substituted alkanethiolate dominates the properties of the interface between the SAM and the contact liquid.⁸⁴ Controlled adsorption of proteins at the SAM surface can be achieved by manipulating this functional head group. Moreover, structural elements that impart selectivity to the Au surface can be incorporated into the SAM. In this manner, antibody (IgG) has been transferred onto a mixed SAM using μ CP. Initially, alkanethiols with different terminal R groups, such as $-\text{COOH}$, $-\text{OH}$ and $-\text{CH}_3$, were self-assembled on Au surfaces by immersing the substrates in ethanolic solutions of thiols or by μ CP. Then, protein was deposited onto the modified Au substrates using μ CP, generating patterns of proteins with micrometre resolution. Tan *et al.* found that the amount of protein transferred to these substrates varied with the mole fraction of polar functionality of the SAM, with a minimum threshold value needed for protein transfer to be carried out. They suggested that the difference in wettability between the stamp and the substrate was the dominant parameter that determined the successful microcontact printing of proteins. Indeed, surface modifications that increase the wettability of the substrate or that decrease the wettability of the stamp were found to expand the types of surfaces that can act as substrates for μ CP of proteins, such as glass or ethylene glycol.⁸²

μ CP routinely produces patterned SAMs with features between 1 μm and several centimetres with edge definition of 50 nm on planar substrates.⁸⁵ However, features as small as 200 nm have been created with edge resolutions better than 50 nm, by optimising the unique fit between the elastomeric stamp with the surface and the rapid reaction of thiols with gold.⁸⁴

5.2. Stamps

Traditionally, stamps used in μ CP are made of elastomeric PDMS, the characteristics of which make it suitable for patterning proteins and cells. It is biocompatible, durable, permeable to gases and can be used with non-planar substrates due to its elasticity.⁷³ However, PDMS is a very hydrophobic material. Proteins require long inking times to form a homogeneous film on hydrophobic stamp surfaces and have a tendency to denature on such surfaces. For these reasons, alternative methods and materials have been studied in order to increase the hydrophilicity of stamp surfaces. One strategy is to treat the PDMS stamps with oxygen plasma. However, the effect of this procedure is only temporary (approx. 1 h). Despite this, Duan *et al.* have developed some novel fabrication strategies using plasma in order to oxidize a PDMS stamp by means of a mask and functionalize the surface using two different silanes, 1H,1H,2H,2H-perfluorodecyltrichlorosilane (PFDTs) and 3-aminopropyl triethoxy-silane (APTS). Three different procedures were used to fabricate bifunctional, flat PDMS stamps. The most efficient method used oxygen plasma to first enhance

the formation of a full PFDTs SAM on the PDMS stamp. Oxygen plasma was again used through a mask to simultaneously remove the PFDTs locally and reactivate the PDMS. Finally, APTS was attached to the surface where the PFDTs had been removed. Such a method using oxygen plasma in two stages resulted in an excellent technique to obtain stamps that could be used with both polar and non-polar inks. However, the numerous steps needed to prepare and cure the stamps does extend fabrication time.⁷⁴

Recently, the advantages of using thermoplastic elastomers as stamps for μ CP of proteins have been demonstrated. A poly(ether-ester) (PEE) consisting of poly(tetramethylene glycol) (PTMG) and poly(butylene terephthalate) (PBT) was used for stamp fabrication to deposit bovine serum albumin (BSA) onto substrate. In comparison to the PDMS stamp, the PEE stamp required shorter inking times and lower ink concentrations to print BSA because of its greater hydrophilicity, which enhanced interactions with protein.⁸⁶ Moreover, the use of such materials decreased the contamination that usually appeared on the patterned substrate due to silicon oligomers transferred from the PDMS stamp. However, there is no method yet reported that has demonstrated a completely clean substrate surface (*e.g.* without any silicon contamination). The presence of silicon oligomer contamination from the PDMS stamp at the surface to be patterned decreases the binding capacity of the micro-contact printed protein, compared to when physically adsorbed to an equivalent surface.⁸³

As with inkjet printing, μ CP offers the possibility of creating patterned structures on non-planar substrates. The process of SAM transfer by μ CP can be done by rolling a gold-coated cylindrical substrate across the surface of the stamp as is shown

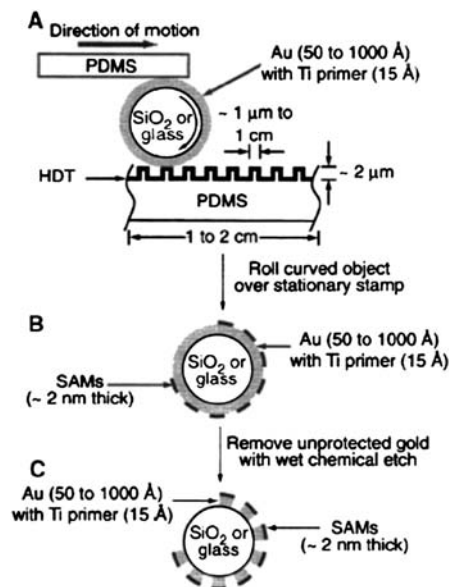


Fig. 10 Schematic process of μ CP on curved surfaces: A) a gold-coated cylindrical substrate is rolled across the surface of the pre-patterned stamp. B) The alkanethiol is only transferred from raised regions of the stamp to the surface of the substrate forming the pattern. C) Gold not protected by SAM can be removed by etching, producing gold microstructures on the curved substrates.⁸⁵

in Fig. 10, or rocking the substrate across the stamp to form the design.

In 1995, Jackman *et al.* reported sub-micrometre features on curved surfaces, achieving feature sizes of about 800 nm on Au-coated cylindrical glass lenses ($r = 5$ cm).⁸⁵ Subsequently, feature linewidths of 175 nm were demonstrated when hexadecanethiol was deposited on planar Ag films and 230 nm on curved surfaces with radii of curvature from 1 to 5 cm.⁸⁷ In terms of fabricating nanostructured features, μ CP has demonstrated itself to be more successful than inkjet printing. Inkjet printing of functional materials is a more recent area of research and it remains to be seen if nanofeatures can be structured with it. However, the drop size in inkjet printing currently limits its use to the micrometer scale, whereas μ CP is limited primarily by the photolithographic technique used to fabricate the mask, which can routinely reach nanodimensions.

Traditionally, materials used to “ink” μ CP stamps were based on alkanethiols. Such compounds are suitable for the formation of SAMs on metallics such as gold, silver and copper. However, applications that require substrates such as glass or oxidized silicon wafers are not compatible with this technique. There have been some recent developments which have made it possible to pattern a variety of materials using silane-based SAMs. Benor *et al.* used a silane-based octadecyltrichlorosilane (OTS) to generate SAMs on silicon wafers and glass surfaces. The surfaces were initially treated with H_2O_2 and H_2SO_4 to render them hydrophilic. Then, a PDMS stamp coated with an OTS ink was brought into contact with the silicon surface. Printed regions were rendered hydrophobic as a result of the Si–O–Si bonds between the OTS molecules and the substrate, while the unexposed regions remained hydrophilic because of the OH-terminated groups created during the cleaning treatment with H_2O_2 and H_2SO_4 . Polymers and resists were selectively deposited in the hydrophilic regions, while the hydrophobic regions did not take up material. The hydrophobic OTS regions were subsequently removed by UV exposure and the resist pattern was used to lift-off different metal films such as chromium and gold. These patterned structures have been used to fabricate a pentacene thin film transistor, in which a resolution of 2 μm was achieved using a polymethyl methacrylate (PMMA) resist.⁷⁵

5.3. Applications

μ CP has been used extensively for the selective deposition of biomolecules (proteins, enzymes and antibodies) in the fabrication of sensor devices. For example, an elastomeric mold containing a pattern of avidin was brought into contact with a surface previously modified with the biotinylated block copolymer, polylactide-poly(ethylene glycol) (PLA-PEG-biotin). The specific interaction between the avidin and the biotin groups permitted binding of biotinylated molecules to the avidin layer, creating a protein pattern.⁷⁷ Poly-L-lysine (PLL) molecules were later deposited onto glass slides, which were initially covered by a plasma-deposited PEG layer. A 1 \times 1 cm of protein-patterned nanoarrays with 300 nm diameter PLL spots and centre-to-centre distances of 500 nm were achieved.⁷⁸ This extension of μ CP to the nanodimension has been referred to as nanotransfer printing (nTP). 70–80 nm features with an edge roughness of 10 nm have also been patterned by exploiting a spontaneous

metallic bonding process that can occur at room temperature between two metal surfaces of like composition by application of pressure known as ‘cold welding’.⁸⁸ In this manner, Kim *et al.* patterned a polymer grating on a SiO_2 surface using gold layers onto both the stamp and the substrate to create the pattern and exploited this technique to fabricate pentacene channel organic thin-film transistors and organic solar cells.⁸⁹

Cell patterning for cell-based biosensors and tissue engineering have generally been carried out using photolithographic techniques to date. However, biocompatibility with photolithographic reagents and the high cost of this method have driven the development of alternative techniques for cell deposition. μ CP has been successfully employed because of its control over the adsorption of proteins, which facilitates the patterning of cells on a range of surfaces with high resolutions. Thus, Rozkiewicz *et al.* reported the deposition of collagen-type proteins by μ CP and the subsequent cell adhesion onto the pre-patterned protein area.⁹⁰ Gold and silicon oxide surfaces were used as substrates, where an amino-terminated SAM was first formed and subsequently modified to obtain an aldehyde-terminated surface. The protein was covalently attached to the aldehyde-terminated substrate creating a well-defined 100- μm spot pattern. After the protein adhesion, the remaining areas were blocked with amino-poly(ethylene glycol) (PEG), which formed a cell-adhesion resistant layer. Human malignant carcinoma (HeLa) cells were then incubated onto the substrate, adhering to the patterned proteins, as is shown in Fig. 11. The size and shape of the cells could be controlled, affecting cell growth and protein secretion. These cell-patterning devices are a platform for the development of cell-based biosensors employed in drug, pathogen and toxin detection.⁹¹

5.4. Other soft lithographic techniques

In addition to conventional μ CP, other soft lithographic techniques include microfluidic network (μ FN), laminar flow and metal transfer (MT) printing.^{11,73} In μ FN printing, microchannels (diameters of 3–200 μm , depending on the material to be patterned) are initially formed on the surface of a PDMS stamp by photolithography. The stamp is then brought into contact with the substrate and the formed microchannels are used to deliver biomolecular ink to the defined areas creating a microfluidic network (μ FN), as is shown in Fig. 12. This method has been used to deposit proteins or cells from a solution

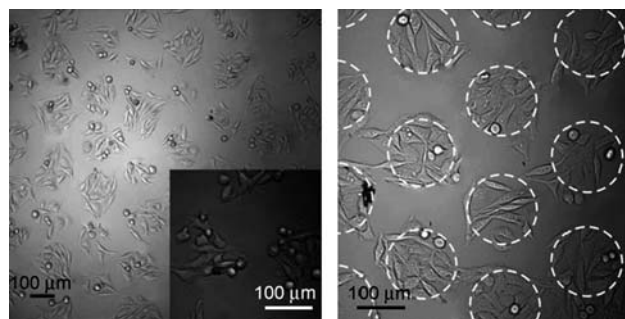


Fig. 11 Patterns of HeLa cells obtained by μ CP of protein col3a1 (100- μm dots separated by 100 μm) into an aldehyde-terminated self-assembled monolayer with polyethylene glycol blocking.⁹⁰

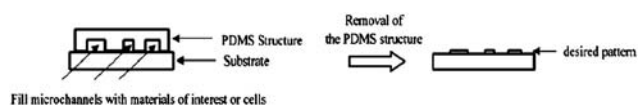


Fig. 12 Schematic process of microfluidic patterning using microchannels. The PDMS stamp is brought into contact with the substrate forming microchannels. Ink is then forced through the channels to create the desired pattern.⁹¹

onto a substrate where the proteins adsorbed in a pattern defined by the microchannels.^{79,91} Microfluidic networks have been created on gold, glass, silicon and polystyrene substrates, reaching feature sizes of approx. 12–70 μm .⁹²

Laminar flow patterning is based on μFN as it uses a microfluidic system in which several inlets converge into a single main channel. The network is created as just described by bringing a pre-patterned PDMS stamp into contact with a substrate such as gold, polystyrene, glass or silicon, obtaining line widths of approx. 10–100 μm . The above-mentioned technique is based on the laminar flow behaviour of liquids in capillaries, which allows two or more layers of fluid to flow next to each other without any mixing other than that taking place by diffusion across the interface. This is illustrated in Fig. 13. The ability to create parallel streams of different biological solutions in capillaries permits cells to be patterned using the typical characteristics of their environment, such as the position of others cells in their vicinity or the fluid medium surrounding them. *E. coli*, erythrocytes and bovine capillary endothelial (BCE) cells have been patterned by Kane and co-workers using the laminar flow technique, achieving the rapid formation of multiple-pattern areas in a single step.⁷³

Metal transfer (MT) printing is another type of μCP , in which a metal layer is deposited on to a polymeric surface. A pre-patterned PDMS stamp created by photolithography is coated with a metal layer which is then transferred to the substrate under heating and slight pressure only where the raised regions of the stamp touch the surface.¹¹ The advantage of this technique over other soft lithographic techniques is that it is rapid (30 s), can pattern large areas in a single pass and can be used to fabricate multi-layered metallic structures. Moreover, as the patterning driving force is the mechanical adhesion between the metal layer

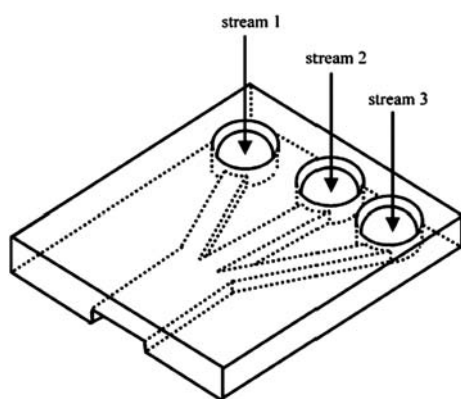


Fig. 13 Scheme of PDMS stamp used in laminar flow patterning. The PDMS microchannel stamp has multiple inlet streams which converge to form parallel flow paths.⁹¹

coated on the PDMS stamp and the surface of the substrate instead of a SAM system, many kinds of metallic materials are suitable for this method, such as gold and aluminium. Thus, a two gold-layer structure (50 μm line width) on a PS/Si substrate was fabricated by MT printing. This technique was then applied to the manufacture of organic field-effect transistors (OFETs).⁹³ Such a method can be applied to the patterning of surfaces with metals, followed by SAMs that will be the sites for proteins to immobilize, serving as an alternate method to conventional μCP .

Grzybowski *et al.* recently developed a technique related to μCP known as wet stamping (WETS).^{94–96} This method uses agarose or polyacrylamide stamps, which have been previously patterned against a PDMS master. The patterned stamps are soaked in an aqueous solution of a patterning reagent which is then brought into contact with a substrate surface, as is shown in Fig. 14. The substrate surface has been pre-treated with a suitable compound designed to react chemically with the ink reagent on the stamp. Upon contact between the stamp and the substrate a microscale chemical reaction-diffusion process occurs between the reagent on the stamp and the substrate, resulting in periodic patterning with potential resolution down to a few nanometres.

This WETS system can be used to etch metallic surfaces by means of a metal dissolution reagent, eliminating the need for a patterned SAM, so the patterned surface can be directly derivatised after etching. In this way, an aqueous solution of trifluoroacetic acid (TFA) was used to microstructure gold films, FeCl_3 -based etchant was used for Cu and Ni films and HNO_3 for Fe surfaces.⁹⁶ In other cases, the precipitation reactions between ions contained within the stamp and compounds placed into a gel on the substrate cause the gels to swell or contract to different degrees, to provide a defined pattern on the surface.⁹⁴ Therefore, WETS offers an alternative to conventional μCP for applications in which reagents are to be delivered to a surface as a solution, as well as the fabrication of microfluidic circuits in glass and

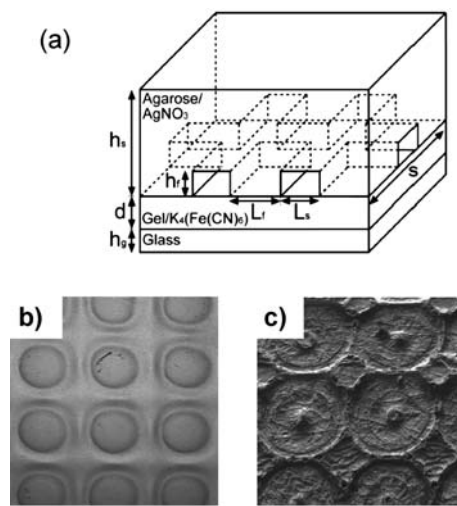


Fig. 14 (a). Experimental setup for patterning AgNO_3 onto thin films of dry gelatine doped with $\text{K}_4\text{Fe}(\text{CN})_6$; (b). Optical micrograph of a non-uniformly swollen gelatine surface 30 s after stamping with an array of circles ($L_s = 100 \mu\text{m}$, $L_f = 100 \mu\text{m}$). Scale bar is 200 μm ; (c). An SEM picture of a UV-cured Norland Optical Adhesive replica of the swollen gel shown in (b).⁹⁴

patterning of metallic membranes. However, the possibility of lateral spreading once the reagents have been stamped limits the resolution of the patterned features, especially if the surface of the stamp is not sufficiently dried before patterning or the surfaces to be patterned are highly hydrophilic.⁹⁵

In summary, μ CP is an innovative technique that is becoming widely used due to its level of sophistication for patterning materials such as proteins and cells. Like inkjet printing, it allows the transfer of a wide variety of materials to a wide array of substrates for patterning. Moreover, μ CP permits the functionalisation of metallic substrates with different terminal group SAMs through covalent thiol-metal bonds, facilitating the selective deposition of materials. Large areas can be patterned in a short time and can obtain greater resolutions (sub-micrometre) than inkjet printing. However, the dependence of a mask as a template to fabricate the stamps increases the time and cost of the production process using this technique, when compared to the maskless approach of inkjet printing. In addition, μ CP also has limitations in the range of substrates which can be used and how the materials must be deposited. It is also heavily reliant on the properties of PDMS which is not suitable in all applications.

6. Probe-based techniques

With the drive towards the miniaturisation of biosensors and other analytical devices, this brings the challenge of moving from the microscale to the nanoscale. The conversion of scanning probe microscopes into modification tools has turned out to be one of the most successful steps forward in the nanopatterning field, setting up a new family of lithographic methods called Scanning Probe Lithographies (SPL). Besides the high resolutions achievable with these techniques (<10 nm), the *in situ* imaging capability enables the visualization of the surfaces while they are being patterned. Dip-pen nanolithography, nano-grafting and local oxidation nanolithography are some of the SPM-based techniques applied for nanopatterning surfaces.

6.1. Dip-pen nanolithography (DPN)

Dip-pen nanolithography (DPN) has recently received increased attention since it was developed by Mirkin *et al.* in 1999.⁹⁷ This technique uses an atomic force microscopy (AFM) tip, modified with a thin film of a chemical of interest, formed by immersing the cantilever in a solution or by evaporation. The coated tip is then brought into contact with the surface to be patterned and the chemical is transferred to it, with molecules flowing from the tip to the sample by capillary action as is shown in Fig. 15. Typical values of contact forces between the AFM tip and the substrate during ink deposition should be 0.3–2 nN in order to avoid damaging the respective surfaces.^{98–100}

Unlike other SPLs that eliminate or modify a passivating layer (*e.g.* by oxidation, etching, shaving or grafting) followed by adsorption of the patterning material, DPN is a direct-write “constructive” lithographic tool, which allows resolutions of <50 nm to be reached.¹⁰¹ The ability to pattern such small features represents one of the main advantages of using DPN. In 1999, Piner *et al.* reported the use of an AFM tip to transfer 1-octadecanethiol molecules to a gold substrate, achieving 30 nm line width resolution.⁹⁷ Although initially these 30 nm width lines

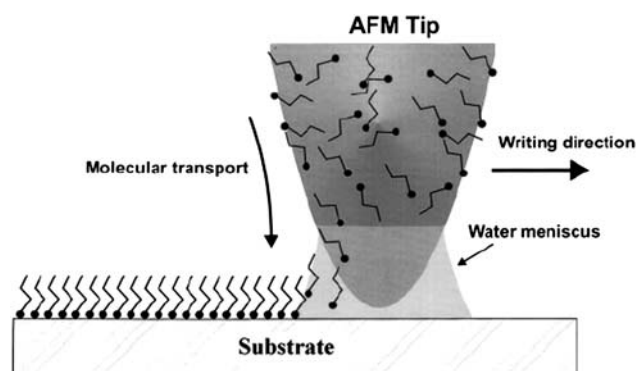


Fig. 15 Schematic representation of the DPN process. A water meniscus forms between the AFM tip coated with “ink” molecules and the solid substrate.⁹⁷

were discontinuous, further studies on the properties of the substrates and tips have enabled improvements in the resolutions and have even allowed the development of protein-based inks. In this way, the spatially controlled patterning of thiolated collagen molecules on a gold substrate using DPN was carried out. Narrow lines of 30–40 nm in width and 100 nm in length were achieved without changing the triple-helical structure and biological activity of collagen.¹⁰²

The resolution of DPN depends on several parameters including the physical properties of the substrate and the scan speed which determines the tip-substrate contact time. Slower scan speeds result in broader lines as it permits a higher number of ink molecules to diffuse to the substrate.⁹⁷ The nature of the ink also plays an essential role in the nanopatterning process and the resolution achievable. The application of different materials as an ink in the DPN process requires characteristics such as homogeneity, low viscosity, slow drying and specific affinity to the substrate. DPN was first used to pattern alkanethiols in 1999, and since then, many inks have been deposited by this technique, such as polymers,^{99,100,103} proteins,^{98,102,104} peptides,^{105,106} colloid particles^{107,108} and metal ions.^{109,110} The molecular transport within the ink between the tip and the substrate is complex and can be influenced by numerous parameters, *e.g.*, the tip shape, surface chemistry, composition and temperature. Moreover, the humidity level under which the experiment is carried out will affect the deposition process by controlling the rate of molecule transport from the tip to the substrate as the dimensions of the water meniscus that bridges the tip and the substrate will be dependent on the relative humidity.^{97,111} This dependence has been shown by means of the creation of different width lines depending on the relative humidity and the contact time between the tip and the substrate.⁹⁷ Therefore, it is necessary to pattern with an AFM encased in a humidity-controlled environmental chamber.

Substrates ranging from metals to insulators have been patterned using DPN. Initially, gold films were used as substrates due to the high affinity shown between the gold and the alkanethiol molecules to be deposited.⁹⁷ More recently, the number of substrates used for this technique has expanded to meet the demands of the newer deposition materials. Modified silicon surfaces have been patterned with conducting polymers,¹⁰³ peptides have been deposited onto GaAs surfaces,¹⁰⁵ gold

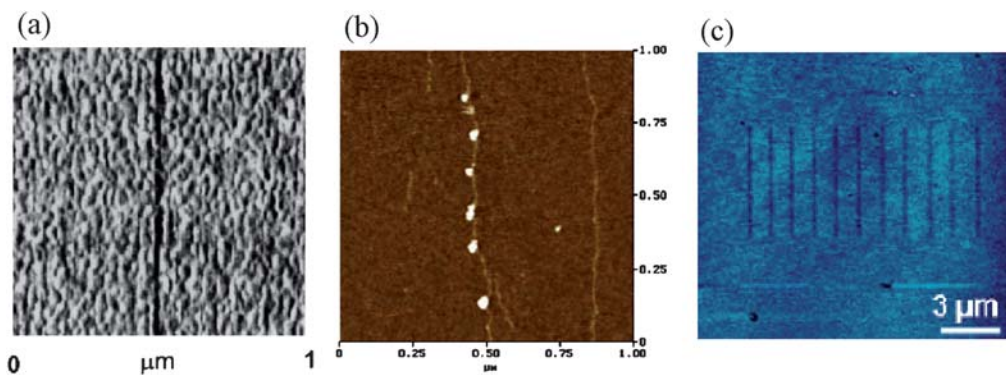


Fig. 16 (a). Lateral force image of a 30 nm-wide line (3 μm long) deposited onto Au/mica by DPN;⁹⁷ (b). AFM image of Cy3-antibody spots along a single DNA molecule;¹⁰⁴ (c). LFM image of GaAs surface patterned with TAT peptide using DPN.¹⁰⁵

colloidal nanoparticles have been patterned on a silicon substrate modified with a layer of phosphorus¹⁰⁷ and even a protein nanopattern has been fabricated along a single DNA molecule¹⁰⁴ as is shown in Fig. 16.

The wide range of inks and substrates associated with DPN yields many applications, such as the study of the fundamental interactions between biological structures and surfaces,^{98,112} sensor development,^{99,113} biomolecular nanoarrays for diagnostic applications¹¹⁴ and manufacture of devices suitable for nanocircuitry.^{101,107,109}

In summary, DPN is a high-resolution patterning tool that allows the fabrication of nanosized features in a wide range of materials. However, its throughput is limited to small-scale production. The parallelization of the DPN technique is the essential development required to bring this technique to production scale and, although several successful approaches have been attempted to engineer the suitable technology required,¹¹⁵ massively parallel and large-area capability are not as yet current DPN characteristics.

6.2. Nanografting

Another AFM-based lithographic method that has permitted patterning at the nanometre size is nanografting. This indirect lithography was introduced in 1997 by Liu *et al.* to fabricate multiple nanostructures that could be rapidly modified and characterized *in situ*.¹¹⁶ Generally, the surfaces to be patterned are gold substrates previously passivated with a resist (such as an alkanethiol SAM) and placed in an AFM fluid cell beneath a solution of the material to be patterned.¹¹⁷

The basic nanografting procedure has three steps as illustrated in Fig. 17. The first step is to characterize the alkanethiol SAM by imaging the surface structure of the matrix with AFM at low force (0.1–1 nN). The second step is to fabricate desired patterns within the SAM. The AFM tip removes SAM molecules in selected areas by scanning these areas at a force just above the threshold displacement force (10–30 nN).¹¹⁸ As the matrix molecules are removed, thiol molecules from the contacting solution immediately adsorb onto these areas creating the patterns. The final step is to characterize the freshly patterned surface using the same AFM tip at a reduced imaging force.

Nanografting was initially used to pattern an alkanethiol SAM matrix (decaneithiol, C_{10}SH) with another alkanethiol of longer

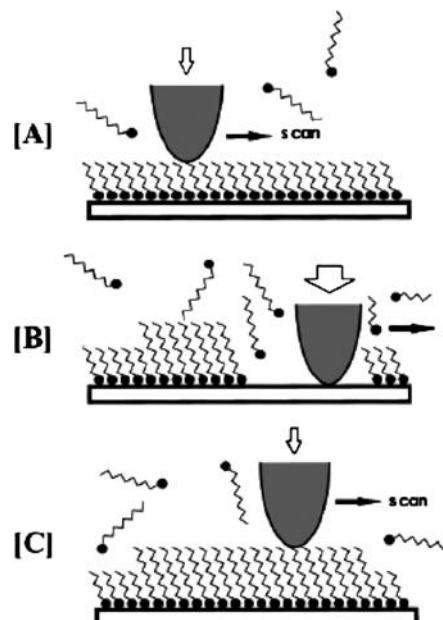


Fig. 17 Schematic diagram of the nanografting procedure illustrating the three main steps of the process. (A) Matrix SAM imaged by AFM at low force. (B) Fabrication of the desired pattern by scanning that area with an AFM tip at a force greater than the displacement threshold. New thiol molecules in the contacting solution attach onto the exposed gold sites. (C) Characterization of the patterned area at a reduced imaging force.¹¹⁹

chain length (octadecanethiol, C_{18}SH) in order to prove the feasibility of this emerging technique as a nanopatterning method. No C_{18}SH – C_{10}SH exchange was observed in the non-patterned area during the experiment showing the high spatial selectivity and precision of nanografting.¹¹⁶ The success obtained in this first approach promoted the use of thiols with a wide range of aliphatic chain lengths (2 to 37) and with functional groups such as $-\text{OH}$, $-\text{CO}_2\text{H}$, $-\text{NH}_2$ and $-\text{CHO}$.¹¹⁹ The patterns were distinguished from the SAM matrix because they exhibited higher friction than the surrounding methyl-terminated matrix in the topographic and frictional force images. These micro-patterned SAMs were used as templates to direct the selective adsorption of protein. For example, Kenseth *et al.* patterned a carboxylic acid terminated thiol into a resist composed of

a methyl-terminated monolayer. The terminal carboxylic group was activated using 1-ethyl-3-(3-dimethylaminopropyl) carbodiimide hydrochloride (EDC) and rabbit IgG antigen was covalently bound to it. The response after the exposure of the device to goat anti-rabbit IgG was assessed by height-based scanning force microscopy. An increase in the average height of 11–12 nm over the thiolate regions was consistent with the specific binding of the antibody to the surface-immobilized antigen.¹²⁰ In order to decrease the non-specific protein adsorption and the use of coupling agents, the same group developed the use of glycol-terminated monolayers as resists and modified fragments of the IgG protein with the functional group –SH (Fab'-SH). Besides IgG, the patterning of other proteins such as bovin serum albumin (BSA) and lysozyme have been explored. The nanografting method was used to incorporate thiols with protein adhesive groups (carboxylate or aldehyde) into a SAM matrix with protein non-adhesive terminal groups, creating the desired patterns. Proteins were then immobilized onto the patterned regions by both covalent and physical adsorption. Covalently attached protein was shown to have a higher stability than the physically adsorbed layers.¹¹⁸ Recently, Hu *et al.* carried out nanografting and characterization of a de novo 4-helix bundle protein onto a gold surface modified with a monolayer of octadecanethiol. The anchoring feature of the engineered protein lay in the Gly-Gly-Cys linker that it possessed as its C-terminus. Such a linker allowed its direct attachment onto the freshly exposed thiol-modified gold surface during the nanografting process, forming protein “islands”. Several parameters related to the technique such as imaging and threshold forces, defective areas, self-reorganization of the protein layers, were studied.¹²¹

As with DPN, several factors can influence the process of nanografting such as scan speed, patterning force and thiol concentration. Slow scan rates produce pattern distortions due to thermal drifts, while fast scan rates produce patterns with lower coverage. Scan rates of around 1–2 $\mu\text{m/s}$ are regularly used in nanografting, resulting in the rapid and reproducible formation of patterns with well-defined geometry and sharp edges.^{119,122} The geometry and chemical nature of AFM tips may vary although generally the cantilevers are made of silicon nitride with a spring constant of 0.1 Nm^{-1} .^{118–120,122} Moreover, it is important to establish the corresponding threshold force required to remove the thiol molecules from the SAM matrix without disturbing the underlying layer of gold. The threshold force is tested by gradually increasing the grafting force until the periodicity changes from that for a thiol monolayer to that for Au (111). Typical load of the AFM tips during the nanografting process is 10–30 nN.^{118,123} Furthermore, by varying the nanografting force, the packing density of the patterned molecules within the nanostructure may be controlled. The effect of adjusting the nanografting force on the packing density of nanostructures of single-stranded DNA (ssDNA) created inside a decanethiol matrix has been reported. The lower the nanografting force applied, the lower the packing density as the AFM tip at low forces cannot remove all resist molecules. In such a way, it was observed that the concentration of the contacting solution containing the compound to be patterned also has an influence on the packing density. When nanografting was conducted at low ssDNA concentrations, the packing density of the patterned compound within the nanostructure was reduced, as is shown in Fig. 18.¹²²

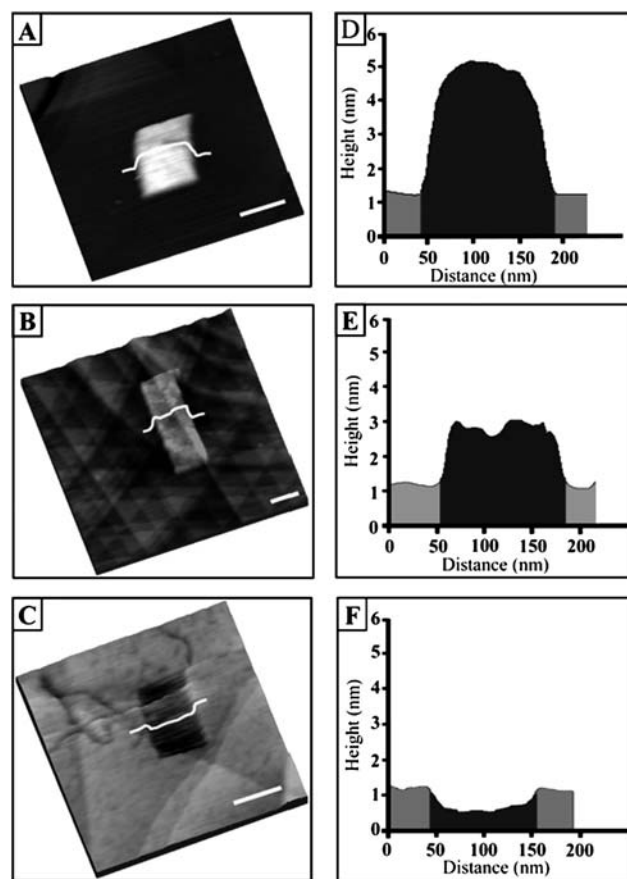


Fig. 18 Nanostructures of 5'-HS-(CH₂)₆(T)₁₅ (oligo T15) with decreasing DNA density. (A) A 120 × 200 nm² nanostructure produced in a T15 solution with a concentration of 40 μM . (B) A 100 × 380 nm² nanostructure produced in a 18 μM T15 solution. (C) A 100 × 200 nm² nanostructure fabricated at T15 concentration of 9 μM . Parts D, E, and F show the corresponding cursor plot as indicated in parts A, B and C.¹²²

Using nanografting, feature sizes as small as 2 × 4 nm (consisting of 32 thiol molecules),¹²⁴ 10 × 150 nm (containing 3 proteins) and 7 × 12 nm with (DNA by-products)^{122,125} have been obtained, achieving an edge resolution of less than 2 nm when octadecanethiol nanolines were produced in a decanethiol matrix.¹¹⁹

A variation of nanografting is the “nanopen reader and writer” technique (NPRW), which combines the advantages of nanografting with dip-pen nanolithography.^{123,124} In NPRW, a SAM serves as the resist, while an AFM tip displaces the resist molecules from desired locations. The AFM tip is pre-coated with adsorbate molecules that can attach to the freshly exposed substrate areas. Unlike nanografting, exchange reactions are prevented as the imaging medium does not contain adsorbate molecules. On the other hand, unlike DPN, resolution is independent of the texture of the substrate and the humidity. Line widths as small as 9 nm have been observed with such a mixed method.¹²³

In short, nanografting results in a simple, fast method of fabricating high density patterned nanostructures as it accelerates the kinetics of the self-assembly of thiolated molecules on gold. The nanografting process creates a spatially confined transient environment, which guides the thiolated molecules to

directly form a “standing-up” configuration instead of adopting a “lying-down” configuration on initial adsorption.¹²²

Compared to other patterning methods such as μ CP, nanografting is a slower tool for mass production of nanostructures. However, it shows much higher resolution (≈ 1 nm edge resolution) than μ CP (≈ 50 nm) and does not require the generation of masks for each pattern or the fabrication of new patterning stamps as in μ CP. It allows fabricated patterns to be altered *in situ*.^{119,121} Moreover, since the imaging and fabrication during the nanografting procedure are carried out in aqueous solution close to physiological conditions, grafted proteins are more likely to retain their bioactivity.^{118,121}

This technique has proven to be a useful tool to study the stability of folded biopolymers in monolayers as well as the structural stability of proteins packed at high density.¹²¹ Moreover, the high precision and pattern resolution obtainable suggest this method to be a reliable process to fabricate protein nanoarrays as well as nanostructures that could be used as components in nanoelectronic devices and sensors.^{119,122}

Another SPM-based nanolithographic method is “local oxidation nanolithography”, which combines the full potential of atomic force microscopes with the application of a bias voltage to pattern multiple materials at the nanoscale. An AFM tip is used here as the cathode to oxidize a wide range of materials (Si, Ti, Al, Cr) by means of the formation of a water meniscus between the tip and the surface to be patterned.^{126,127} This technique has been mainly used in the development of nanoelectronic devices, as Snow & Campbell demonstrated by fabricating metal wires and metal-oxide-metal junctions with sub-10 nm sizes and high precision.¹²⁸ Most recently, some attempts of applying local oxidation nanolithography to pattern biomolecules have been made.¹²⁹ However, no results as successful as those obtained with other AFM-based techniques have yet been reported, possibly due to the application of the high bias potential required during the patterning process.

7. Lithographic techniques (photolithography, electron beam and laser-assisted deposition)

Different radiation sources, such as light, X-ray or electron beam (e-beam), have been used as patterning devices for protein deposition procedures, creating a desired pattern onto a resist material previously coated to a substrate. Two methods have shown particular strengths for patterning materials and biomaterials: photolithography and e-beam. During the photolithographic process, a collimated light passes through a mask generating a latent image of the mask in a thin film of polymer resist deposited *via* spin-coating.^{88,130} Then, the substrate is treated with a suitable solvent to dissolve either the radiation-exposed areas (positive resist) or the unexposed areas (negative resist), creating the appropriate surface onto which the proteins will be deposited.⁸⁸ Whereas the first generation of resists was based on phenol-formaldehyde polymers, modern resists combine onium salts with poly(4-[t-butylloxycarbonyl-oxy]styrene) or are based on epoxy polymers such as SU-8 resists which are much more sensitive and versatile.¹³⁰ The typical limit of resolution for standard photolithography is several micrometers (1–5 μ m).^{131,132} However, the fabrication of 0.8 μ m size patterns has recently been achieved by decreasing the photoresist

thickness to 0.13 μ m from 1 μ m and using a second masking layer of silica with high etching selectivity.¹³¹

Bovine serum albumin (BSA) and horseradish peroxidase (HRP) were also micropatterned onto glass-silica substrates by photolithography. The substrate was coated with a commercial positive photoresist before it was illuminated by light (364 nm) transmitted through a photolithographic mask. The sample was then immersed in solvent to remove the exposed resist and create a suitable environment for protein deposition. HRP was shown to retain its catalytic activity after patterning by means of the positive test with diaminobenzidine (DAB) in the presence of H_2O_2 . Protein line-widths of approx. 1.5 μ m were achieved.¹³³ Taguenang *et al.* reported an enhancement of the hydrophilicity of poly-L-lysine (PLL) films after they were exposed through the mask to deep UV light. The increased surface roughness and porosity created by UV irradiation was investigated by observing adsorption of ambient humidity when the substrate was placed in a stream of water vapour saturated air. Higher condensation of ambient moisture was shown only over UV-exposed areas. Hydrophobic microspheres of gold and polystyrene were then selectively attached to areas not previously exposed to UV light, creating micro-/nano-porous arrays. Adsorption of microspheres to surfaces is widely used to bind antibodies for biological applications, whereas porous substrates are used to microencapsulate biological molecules or as a matrix for supporting catalysts.¹³⁴

Matrix-assisted pulsed laser evaporation (MAPLE) is, as the name suggests, a laser-based photolithographic technique which allows the deposition of biomolecules. The incident laser initiates a photothermal process in a frozen water matrix, vaporizing the frozen material and releasing the biomolecule into the chamber as is shown in Fig. 19. Because of the low concentration of biomaterial in the target, the photons interact primarily with the matrix, and the macromolecules are released undamaged and are directed onto the substrate due to the momentum resulting after the vaporization. Such a non-destructive procedure was carried out to fabricate thin films of active enzyme HRP with thicknesses between 10 nm and 1 μ m. The same procedure in the presence of a photomask was used to form patterns of an HRP/PEG composite with 20–250 μ m diameters. The activity of the enzyme after modification was measured by the exposure of the substrate to a solution containing H_2O_2 and DAB. The production of a dark-coloured precipitate was a clear indication that the protein maintained its activity after the MAPLE procedure.¹³⁵

Techniques involving laser applications for biomolecule deposition are becoming widely used, notwithstanding their apparent complexity, as they solve the problem of multistep procedures enabling the direct writing of biomaterials. In this way, HRP and Immunoglobulin G were deposited on silicon substrates by laser-assisted technique, with the retention of protein activity following the process. Very uniform and thin protein layers (approx. 5 nm) were obtained after measuring their roughness by means of an AFM tip. Subsequently, $0.5 \times 2 \mu\text{m}^2$ patterns were created onto the previously laser-assisted deposited layer of peroxidase by e-beam lithography and lift-off.¹³⁶ The feasibility of this technique to fabricate biomolecule arrays has also been proven. *Treponema pallidum* 17 kDa protein antigens were deposited on a glass slide as the basis of a diagnostic kit for syphilis in human patients. The antigen solution was spread on

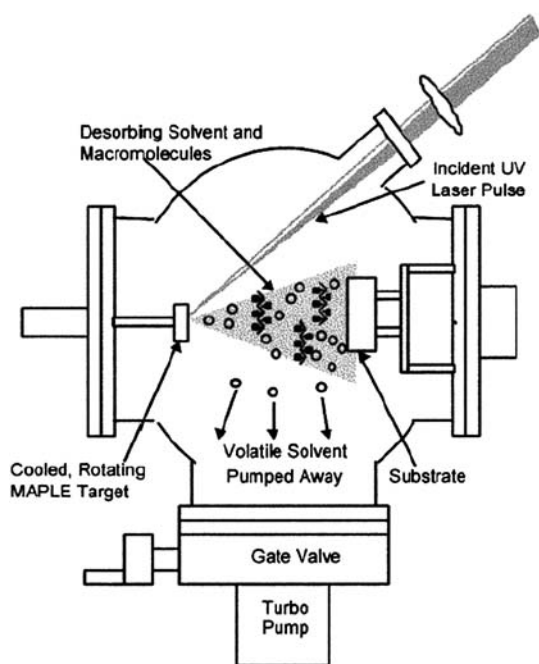


Fig. 19 Schematic of MAPLE apparatus. The incident laser pulse is focused on the frozen target consisting of a dilute mixture of biomolecule in an aqueous buffer solution. The laser energy is absorbed by the matrix (water molecules), resulting in desorption of both water and biomolecules. The more volatile water is pumped away by the vacuum, and the less volatile biomaterial is captured by the substrate, forming a pure film of active material.¹³⁵

a Ti film that coated a glass substrate. The microarrays were created by applying a pulsed Nd:YAG laser beam (355 nm wavelength, 10 ns pulse duration) onto the Ti film, providing 10×10 spots microarrays of antigen, which conserved its immunological reactivity following transfer.¹³⁷ Other biological materials already deposited by laser-assisted techniques are DNA,¹³⁸ cells^{139,140} and tissues.¹⁴⁰

The photomasks (generally comprised of metallic substances such as nickel mesh or chromium^{88,134}) used in photolithography and laser-assisted methods are usually fabricated by e-beam lithography. This is a maskless technique that uses an electron beam to scan across the surface, generating nano-sized features.^{88,132,141,142} In this way, glucose and glutamine-binding protein isolated from *E. coli* and sugar-binding protein isolated from *Pyrococcus horikoshii* have been deposited onto a pre-patterned irradiated material, retaining their biological activity.¹⁴³ As a substrate, they used electrochemically-obtained porous silicon (PS), which was electron irradiated using a Scanning Electron Microscope (SEM) as the source of the beam current. Protein solution was deposited on the samples by a micropipette and left to incubate, allowing proteins to specifically bind to the irradiated PS as the electron beam provoked the generation of silicon radicals and, therefore, a strong localized reactivity on the PS substrate. It was also observed that the number of molecules binding the material varied with the incubation time in the protein solution and the accelerating voltage used in the SEM.

Song *et al.* compared photolithographic and e-beam methods by the fabrication of diamond solution-gate field-effect

transistors (SGFETs). The channel length achieved with photolithography was 5 μm whereas submicron-sized channels (500 nm) were obtained with e-beam. The smaller the channel length, the higher the transconductance and thus the sensitivity of the FET-type amperometric biosensor created after the immobilization of the desired enzyme on the amine-functionalized channel surface.¹³²

This technique can be also used to create polymeric structures in the micrometer range.¹⁴⁴ Flexible poly(tetrafluoroethylene-co-ethylene) (ETFE) substrates were irradiated with an e-beam and then grafted in an aqueous solution of acrylic acid. Lines of 1.7 μm wide and 150 nm high were measured by AFM imaging of the surface, as is shown in Fig. 20.

E-beam lithography is a slow technique and therefore not as suited to mass-production operations when compared to photolithography. In terms of speed, no lithographic method compares to non-optical patterning methods, such as ink-jet printing or microcontact printing. Moreover, lithography tends to have low resolution (micron-size) and is restricted to planar substrates. However, the photolithographic MAPLE presents the unique ability of forming multilayers of many different materials, which would permit the manufacture of all the components of biosensors (electrodes, biological molecules, polymer, biomaterial protecting layer, *etc*) by the use of this technique.¹³⁵ Furthermore, e-beam seems to be a suitable option for prototyping, low-volume work and mask production or repair.

In short, although the above-mentioned lithographic methods are not yet the best directly applicable techniques for mass production of biosensors, they play important complementary roles in initial steps of the manufacture. For example, polymeric pre-patterned stamps used in μCP to transfer materials onto substrates are fabricated by exposure to UV light through a mask, which is fabricated by optical lithographic techniques. Stencil masks used for surface patterning in screen-printing are also created by photoetching methods. Therefore, the sharpness and the resolution of devices manufactured by techniques such as μCP or screen-printing will be determined by optical lithographic methods.

8. Plasma-based patterning

Biosensors typically consist of biological components immobilised to transducers, so improving the intimate connection

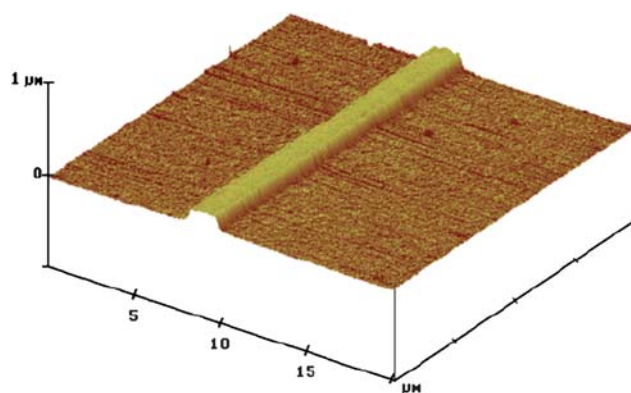


Fig. 20 AFM image of a line structure generated by e-beam irradiation of an ETFE film followed by grafting with acrylic acid.¹⁴⁴

between them emerges as a key factor in device performance. Plasma polymerization has been developed for the deposition of thin and well-packed films used as interfacial layers in biosensor manufacture.

Briefly, the plasma polymerization process begins with the supply of gas or liquid monomers from their respective containers (bombs or liquid reservoirs) to the chamber where polymerization itself will be carried out. The monomers are vaporized and the chamber is filled by controlling the pressure and flow rate. Then, electromagnetic power is supplied to generate active species for polymerization and glow discharge occurs. The thin film is subsequently deposited onto the substrate surface with a typical deposition rate of 100–1000 nm/min. The parameters for plasma polymerization are discharge power and frequency, monomer structure, reactor type, flow rate of monomer, plasma pressure and substrate temperature and position. A range of surface functionalities, such as amino, thiol, carboxyl and hydroxyl groups, can be achieved depending on the plasma gas applied.^{145,146}

Thin films were fabricated by plasma polymerization of 2-amino-benzotrifluoride, acrylic or methacrylic acid, which functionalised the substrate with amino and carboxylic groups. As a substrate thin film noble metal electrodes (gold or platinum) deposited by vacuum evaporation on silicon surfaces were used. Following this, plasma treatment of the surface using ammonia or oxygen plasma was shown to increase the amount of functionalized groups. After chemical activation of the amino and carboxyl groups, glucose oxidase (GOx) was immobilized on the

surface, and its activity was measured by electrochemical methods, creating an amperometric biosensor for glucose detection.¹⁴⁷ Since then, several groups have developed glucose sensors by means of plasma polymerized thin film deposition. Yoshimura *et al.* carried out the encapsulation of GOx in a membrane with subsequent plasma polymerization in order to avoid possible interferences from the sample solution.^{148,149} Muguruma *et al.* incorporated dimethylaminomethylferrocene (DMAMF) as a mediator into the plasma-polymerized film that coated the immobilized GOx, as is shown in Fig. 21. The first 10 nm thick layer only partially covered the adsorbed enzyme, which was evident by the contour of the GOx in the AFM image 21c. When the thickness was increased to 20 nm (Fig. 21d), the enzyme was completely coated. One problem related to the leaching of the redox mediator out of the matrix was prevented by multiple CV scans before the use of the device. When the amperometric background current reached a steady state (following expulsion of residual redox monomer from the film), the device was ready for its application. Electrochemical measurements of the system showed a high increase in anodic current when glucose was added to the solution, indicating that a successful electron transfer mechanism had been created.¹⁵⁰

The plasma polymerization technique has also been used to fabricate other types of biosensors, such as potentiometric,^{122,151} or capacitance¹⁵² measuring devices as well as immunosensors^{153–156} and nucleic-acid^{157,158} sensors in combination with quartz crystal microbalance (QCM) and surface plasmon resonance (SPR) or Bio-MicroElectroMechanical Systems (BioMEMS).

Although several groups have reported the use of a mask to pattern surfaces by the plasma-polymerization method,¹⁴⁷ most of them utilized this technique to functionalize substrate surfaces to improve the immobilization of the enzymes. Moreover, the use of vacuum during the process makes its industrial application expensive. However, this technique could be used as a complementary method together with any other patterning technique in order to improve the enzymatic adhesion to pre-patterned structures.

9. Conclusions

The interaction of different areas of microsystems technology, traditional printing techniques, nanotechnology and the physical sciences enables the fabrication of custom-made devices by the application of a huge range of patterning techniques, as has been demonstrated. Most of the methods discussed have been used for the deposition of biological compounds (proteins, enzymes, DNA) onto multiple substrates in order to develop sensing devices. However, the application of these techniques was not always used for the direct immobilization of these materials, but was used to pattern the substrate surfaces and subsequently deposit the biological molecules from a solution. Thus, enzymes have been directly^{19,135} and indirectly^{39,133} deposited by inkjet printing and lithographic methods whereas plasma polymerization was only used for indirect deposition^{147,150} due to the extreme conditions required during its application. Some of the scanning-probe-based techniques such as dip-pen nanolithography and local oxidation have also enabled the direct deposition of protein and enzymes, whereas nanografting has only allowed their indirect immobilization due to its destructive

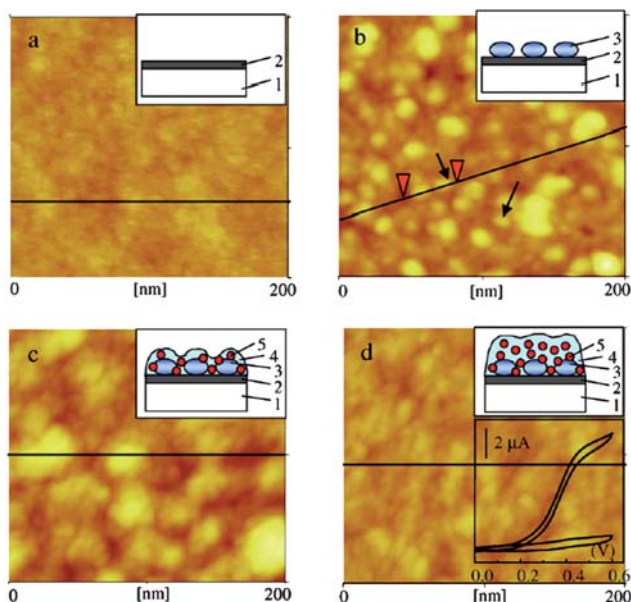


Fig. 21 Tapping-mode AFM images of plasma-polymerized film (PPF). (a) Pristine surface of a hexamethyldisiloxane (HMDS) PPF. (b) After physisorption of GOx. (c) Following addition of a 10-nm-thick DMAMF PPF overcoating to the GOx-adsorbed surface. (d) Following addition of a 20-nm DMAMF PPF overcoating. Upper insets: schematics of enzyme-electrode construction. 1: Sputtered Au-electrode; 2: HMDS PPF; 3: GOx; 4: DMAMF PPF overcoating; 5: Ferrocene. Lower inset in (d): Cyclic voltammograms of the electrode of GOx overcoated with DMAMF PPF in absence and presence of 41.7 mM glucose.¹⁵⁰

nature. Proteins, enzymes and human cells have all been patterned onto substrates by inkjet printing (direct approach) or microcontact printing (indirect deposition).

With regards to mass-production, inkjet printing seems to be a very promising technique as it combines the ability to deposit a huge range of materials through a non-contact mechanism and does not require a mask. However, the micrometer-size resolution limits its application when nano-scale features are desired. In such cases, scanning probe lithographies are more useful, allowing the visualization of the patterned areas, although the time-consuming nature of the procedure is a drawback for industrial application. Microcontact printing, on the other hand, allows patterning of large surfaces (flat and curves) in a short time, but with the requirement of a mask to pre-pattern the printing stamp.

In summary, an ideal technique which allows mass-production of nanometer-sized patterns in a short time frame with high precision does not currently exist. Using just one patterning technique means choosing which characteristics of the final devices are most important (e.g. cost, resolution, etc). However, combining two or more of the techniques discussed could result in a more optimal methodology for the fabrication and production of devices with highly specific characteristics. No doubt future developments of these technologies will eventually lead to high throughput and high precision in a single production process.

References

- 1 L. Setti, A. Fraleoni-Morgera, B. Ballarin, A. Filippini, D. Frascaro and C. Piana, *Biosens. Bioelectron.*, 2005, **20**, 2019–2026.
- 2 O. Ngamna, A. Morrin, A. J. Killard, S. E. Moulton, M. R. Smyth and G. G. Wallace, *Langmuir*, 2007, **23**, 8569–8574.
- 3 K. Crowley, E. O'Malley, A. Morrin, M. R. Smyth and A. J. Killard, *Analyst*, 2008, **133**, 391–399.
- 4 T. Sekitani, Y. Noguchi, U. Zschieschang, H. Klauk and T. Someya, *Proc. Natl. Acad. Sci. U. S. A.*, 2008, **105**, 4976–4980.
- 5 K. Murata, J. Matsumoto, A. Tezuka, Y. Matsuba and H. Yokoyama, *Microsystem Technologies-Micro-and Nanosystems-Information Storage and Processing Systems*, 2005, **12**, 2–7.
- 6 P. H. Chen, W. C. Chen and S. H. Chang, *International Journal of Mechanical Sciences*, 1997, **39**, 683.
- 7 L. Setti, C. Piana, S. Bonazzi, B. Ballarin, D. Frascaro, A. Fraleoni-Morgera and S. Giuliani, *Anal. Lett.*, 2004, **37**, 1559–1570.
- 8 B. Ballarin, A. Fraleoni-Morgera, D. Frascaro, S. Marazzita, C. Piana and L. Setti, *Synth. Met.*, 2004, **146**, 201–205.
- 9 S. B. Fuller, E. J. Wilhelm and J. A. Jacobson, *J. Microelectromech. Syst.*, 2002, **11**, 54–60.
- 10 L. Lin and X. Bai, *Pigm. Resin Technol.*, 2004, **33**, 238–244.
- 11 R. Parashkov, E. Becker, T. Riedl, H. H. Johannes and W. Kowalsky, *Proc. IEEE*, 2005, **93**, 1321–1329.
- 12 J. D. Newman, A. P. F. Turner and G. Marrazza, *Anal. Chim. Acta*, 1992, **262**, 13–17.
- 13 S. Magdassi and M. Ben Moshe, *Langmuir*, 2003, **19**, 939–942.
- 14 T. Xu, J. Jin, C. Gregory, J. J. Hickman and T. Boland, *Biomaterials*, 2005, **26**, 93–99.
- 15 G. M. Nishioka, A. A. Markey and C. K. Holloway, *J. Am. Chem. Soc.*, 2004, **126**, 16320–16321.
- 16 N. Y. Sabina Di Risio, *Macromol. Rapid Commun.*, 2007, **28**, 1934–1940.
- 17 U. S. S. Berend-Jan de Gans, *Macromol. Rapid Commun.*, 2003, **24**, 659–666.
- 18 L. Lonini, D. Accoto, S. Petroni and E. Guglielmini, *J. Biochem. Biophys. Methods*, 2008, **70**, 1180–1184.
- 19 A. Roda, M. Guardigli, C. Russo, P. Pasini and M. Baraldini, *Biotechniques*, 2000, **28**, 492–496.
- 20 L. R. Allain, M. Askari, D. L. Stokes and T. Vo-Dinh, *Fresenius J. Anal. Chem.*, 2001, **371**, 146–150.
- 21 T. Okamoto, T. Suzuki and N. Yamamoto, *Nat. Biotechnol.*, 2000, **18**, 438–441.
- 22 Y. Kim, S. Son, J. Choi, D. Bym and S. Lee, *J. Semic. Tech. Sci.*, 2008, **8**, 121–127.
- 23 S. Shigematsu, Y. Ishida, N. Nakashima and T. Asano, *Jpn. J. Appl. Phys.*, 2008, **47**, 5109–5112.
- 24 K. E. Paul, W. S. Wong, S. E. Ready and R. A. Street, *Appl. Phys. Lett.*, 2003, **83**, 2070–2072.
- 25 P. Calvert, *Chem. Mater.*, 2001, **13**, 3299–3305.
- 26 A. M. J. van den Berg, A. W. M. de Laat, P. J. Smith, J. Perelaer and U. S. Schubert, *J. Mater. Chem.*, 2007, **17**, 677–683.
- 27 D. Soltman and V. Subramanian, *Langmuir*, 2008, **24**, 2224–2231.
- 28 H. Irringhaus, T. Kawase, R. H. Friend, T. Shimoda, M. Inbasekaran, W. Wu and E. P. Woo, *Science*, 2000, **290**, 2123–2126.
- 29 B. L. Groenendaal, F. Jonas, D. Freitag, H. Pielartzik and J. R. Reynolds, *Adv. Mater.*, 2000, **12**, 481–494.
- 30 B. Chen, T. H. Cui, Y. Liu and K. Varshney, *Solid-State Electron.*, 2003, **47**, 841–847.
- 31 J. P. H. Lima and A. M. de Andrade, *J. Mater. Sci.: Mater. Electron.*, 2006, **17**, 593–596.
- 32 R. B. Rakhii, K. Sethupathi and S. Ramaprabhu, *Appl. Surf. Sci.*, 2008, **254**, 6770–6774.
- 33 S. Ghosh and O. Inganas, *Synth. Met.*, 1999, **101**, 413–416.
- 34 M. Onoda, K. Tada and H. Nakayama, *Japanese Journal of Applied Physics Part 1-Regular Papers Short Notes & Review Papers*, 1999, **38**, 3736–3741.
- 35 Z. N. Bao, Y. Feng, A. Dodabalapur, V. R. Raju and A. J. Lovinger, *Chem. Mater.*, 1997, **9**, 1299.
- 36 S. A. Waghuley, S. M. Yenorkar, S. S. Yawale and S. P. Yawale, *Sens. Actuators, B*, 2008, **128**, 366–373.
- 37 A. Morrin, F. Wilbeer, O. Ngamna, S. E. Moulton, A. J. Killard, G. G. Wallace and M. R. Smyth, *Electrochem. Commun.*, 2005, **7**, 317–322.
- 38 P. J. Smith, D. Y. Shin, J. E. Stringer, B. Derby and N. Reis, *J. Mater. Sci.*, 2006, **41**, 4153–4158.
- 39 M. S. Hasenbank, T. Edwards, E. Fu, R. Garzon, T. F. Kosar, M. Look, A. Mashadi-Hossein and P. Yager, *Anal. Chim. Acta*, 2008, **611**, 80–88.
- 40 A. Bietsch, J. Y. Zhang, M. Hegner, H. P. Lang and C. Gerber, *Nanotechnology*, 2004, **15**, 873–880.
- 41 R. E. Saunders, J. E. Gough and B. Derby, *Biomaterials*, 2008, **29**, 193–203.
- 42 R. E. Saunders, J. E. Gough and B. Derby, *Nanoscale Materials Science in Biology and Medicine*, Warrendale, PA 2005.
- 43 P. Calvert, *Science*, 2007, **318**, 208–209.
- 44 S. K. Hwang, K. D. Lee and K. H. Lee, *Jpn. J. Appl. Phys.*, 2001, **40**, L580–L582.
- 45 M. Albareda-Sirvent, A. Merkoci and S. Alegret, *Sens. Actuators, B*, 2000, **69**, 153–163.
- 46 M. Tudorache and C. Bala, *Anal. Bioanal. Chem.*, 2007, **388**, 565–578.
- 47 S. Kaimori, T. Kitamura, M. Ichino, T. Hosoya, F. Kurusu, T. Ishikawa, H. Nakamura, M. Gotoh and I. Karube, *Anal. Chim. Acta*, 2006, **573**, 104–109.
- 48 K. Grennan, A. J. Killard and M. R. Smyth, *Electroanalysis*, 2001, **13**, 745–750.
- 49 M. Gutierrez, V. M. Moo, S. Alegret, L. Leija, P. R. Hernandez, R. Munoz and M. del Valle, *Microchim. Acta*, 2008, **163**, 81–88.
- 50 D. H. Lee, J. S. Choi, H. Chae, C. H. Chung and S. M. Cho, *Curr. Appl. Phys.*, 2009, **9**, 161–164.
- 51 Y. D. Tanimoto de Albuquerque and L. F. Ferreira, *Anal. Chim. Acta*, 2007, **596**, 210–221.
- 52 J. Razumiene, J. Barkauskas, V. Kubilius, R. Meskys and V. Laurinavicius, *Talanta*, 2005, **67**, 783–790.
- 53 R. M. Pemberton, R. Pittson, N. Biddle, G. A. Drago and J. P. Hart, *Anal. Lett.*, 2006, **39**, 1573–1586.
- 54 M. Boujitta, J. P. Hart and R. Pittson, *Biosens. Bioelectron.*, 2000, **15**, 257–263.
- 55 A. E. A. C. Hakan Karadeniz, *Electroanalysis*, 2008, **20**, 1932–1938.
- 56 J. Wang, P. V. A. Pamidi and K. R. Rogers, *Anal. Chem.*, 1998, **70**, 1171–1175.
- 57 J. Wang and X. J. Zhang, *Anal. Lett.*, 1999, **32**, 1739–1749.

- 58 E. Crouch, D. C. Cowell, S. Hoskins, R. W. Pittson and J. P. Hart, *Anal. Biochem.*, 2005, **347**, 17–23.
- 59 V. Guidi, M. A. Butturi, M. C. Carotta, B. Cavicchi, M. Ferroni, C. Malagù, G. Martinelli, D. Vincenzi, M. Sacerdoti and M. Zen, *Sens. Actuators, B*, 2002, **84**, 72–77.
- 60 P. S. More, Y. B. Kholam, S. B. Deshpande, S. K. Date, N. D. Sali, S. V. Bhoraskar, S. R. Sainkar, R. N. Karekar and R. C. Aiyer, *Mater. Lett.*, 2004, **58**, 1020–1025.
- 61 T. A. R. Skotheim, J.R., *Conjugated Polymers: Processing & Applications*, 2nd edn, CRC Press, 1998.
- 62 S.M.Y., S. A. Waghuley, S. S. Yawale and S. P. Yawale, *Sensors and Transducers Journal*, 2007, **79**, 1180–1185.
- 63 H. Santa-Nokki, J. Kallioinen, T. Kololuoma, V. Tuboltsev and J. Korppi-Tommola, *J. Photochem. Photobiol., A*, 2006, **182**, 187–191.
- 64 E. J. Widjaja, G. Delporte, F. Vandeveldel and B. Vanterwyngen, *Sol. Energy Mater. Sol. Cells*, 2008, **92**, 97–100.
- 65 D. W. Li and L. J. Guo, *Journal of Physics D-Applied Physics*, 2008, **41**.
- 66 T. Makela, T. Haatainen, P. Majander and J. Ahopelto, *Microelectron. Eng.*, 2007, **84**, 877–879.
- 67 M. Tuomikoski, R. Suhonen, M. Valimakia, T. Maaninen, A. Maaninen, M. Sauer, P. Rogin, M. Mennig, S. Heusing, J. Puetz and M. A. Aegerter, *Organic Optoelectronics and Photonics II*, 2006, **6192**, 19204–19204.
- 68 T. Haatainen, P. Majander, T. Riekkinen and J. Ahopelto, *Microelectron. Eng.*, 2006, **83**, 948–950.
- 69 T. Makela, T. Haatainen, P. Majander, J. Ahopelto and V. Lambertini, *Jpn. J. Appl. Phys.*, 2008, **47**, 5142–5144.
- 70 US Pat., 2008.
- 71 , 2005.
- 72 United States Pat., 2004.
- 73 R. S. Kane, S. Takayama, E. Ostuni, D. E. Ingber and G. M. Whitesides, *Biomaterials*, 1999, **20**, 2363–2376.
- 74 X. X. Duan, V. B. Sadhu, A. Perl, M. Peter, D. N. Reinhoudt and J. Huskens, *Langmuir*, 2008, **24**, 3621–3627.
- 75 A. Benor and D. Knipp, *Org. Electron.*, 2008, **9**, 209–219.
- 76 D. Falconnet, A. Koenig, T. Assi and M. Textor, *Adv. Funct. Mater.*, 2004, **14**, 749–756.
- 77 N. Patel, R. Bhandari, K. M. Shakesheff, S. M. Cannizzaro, M. C. Davies, R. Langer, C. J. Roberts, S. J. B. Tendler and P. M. Williams, *J. Biomater. Sci., Polym. Ed.*, 2000, **11**, 319–331.
- 78 A. Ruiz, A. Valesia, F. Bretagnol, P. Colpo and F. Rossi, *Nanotechnology*, 2007, **18**.
- 79 A. Bernard, J. P. Renault, B. Michel, H. R. Bosshard and E. Delamarche, *Adv. Mater.*, 2000, **12**, 1067–1070.
- 80 C. L. Feng, A. Embrechts, I. Bredebusch, J. Schnekenburger, W. Domschke, G. J. Vancso and H. Schonherr, *Adv. Mater.*, 2007, **19**, 286.
- 81 A. Kumar and G. M. Whitesides, *Appl. Phys. Lett.*, 1993, **63**, 2002–2004.
- 82 J. L. Tan, J. Tien and C. S. Chen, *Langmuir*, 2002, **18**, 519–523.
- 83 J. O. Foley, E. Fu, L. J. Gamble and P. Yager, *Langmuir*, 2008, **24**, 3628–3635.
- 84 M. Mrksich and G. M. Whitesides, *TIBTECH*, 1995, **13**, 228–235.
- 85 R. J. Jackman, J. L. Wilbur and G. M. Whitesides, *Science*, 1995, **269**, 664–666.
- 86 D. C. Trimbach, H. Stapert, J. Van Orselen, K. D. Jandt, C. W. M. Bastiaansen and D. J. Broer, *Adv. Eng. Mater.*, 2007, **9**, 1123–1128.
- 87 D. M. Longo, W. E. Benson, T. Chraska and R. Hull, *Appl. Phys. Lett.*, 2001, **78**, 981–983.
- 88 M. E. Stewart, M. J. Motala, J. Yao, L. B. Thompson and R. G. Nuzzo, *Proc. ImechE, Part N: J. Nanoeng. Nanosyst.*, 2007, **220**, 81–138.
- 89 C. Kim, M. Shtein and S. R. Forrest, *Appl. Phys. Lett.*, 2002, **80**, 4051–4053.
- 90 D. I. Rozkiewicz, Y. Kraan, M. W. T. Werten, F. A. de Wolf, V. Subramaniam, B. J. Ravoo and D. N. Reinhoudt, *Chem.–Eur. J.*, 2006, **12**, 6290–6297.
- 91 T. H. Park and M. L. Shuler, *Biotechnol. Prog.*, 2003, **19**, 243–253.
- 92 N. Patel, R. Padera, G. H. W. Sanders, S. M. Cannizzaro, M. C. Davies, R. Langer, C. J. Roberts, S. J. B. Tendler, P. M. Williams and K. M. Shakesheff, *Faseb Journal*, 1998, **12**, 1447–1454.
- 93 Z. Wang, J. F. Yuan, J. Zhang, R. B. Xing, D. H. Yan and Y. C. Han, *Adv. Mater.*, 2003, **15**, 1009.
- 94 C. J. Campbell, R. Klajn, M. Fialkowski and B. A. Grzybowski, *Langmuir*, 2005, **21**, 418–423.
- 95 C. J. Campbell, S. K. Smoukov, K. J. M. Bishop and B. A. Grzybowski, *Langmuir*, 2005, **21**, 2637–2640.
- 96 S. K. Smoukov, K. J. M. Bishop, R. Klajn, C. J. Campbell and B. A. Grzybowski, *Adv. Mater.*, 2005, **17**, 1361.
- 97 R. D. Piner, J. Zhu, F. Xu, S. H. Hong and C. A. Mirkin, *Science*, 1999, **283**, 661–663.
- 98 M. Lee, D. K. Kang, H. K. Yang, K. H. Park, S. Y. Choe, C. Kang, S. I. Chang, M. H. Han and I. C. Kang, *Proteomics*, 2006, **6**, 1094–1103.
- 99 Q. Tang and S. Q. Shi, *Sens. Actuators, B*, 2008, **131**, 379–383.
- 100 M. Su, M. Aslam, L. Fu, N. Q. Wu and V. P. Dravid, *Appl. Phys. Lett.*, 2004, **84**, 4200–4202.
- 101 K. Salaita, Y. H. Wang and C. A. Mirkin, *Nat. Nanotechnol.*, 2007, **2**, 145–155.
- 102 D. L. Wilson, R. Martin, S. Hong, M. Cronin-Golomb, C. A. Mirkin and D. L. Kaplan, *Proc. Natl. Acad. Sci. U. S. A.*, 2001, **98**, 13660–13664.
- 103 J. H. Lim and C. A. Mirkin, *Adv. Mater.*, 2002, **14**, 1474.
- 104 B. Li, Y. Zhang, J. Hu and M. Q. Li, *Ultramicroscopy*, 2005, **105**, 312–315.
- 105 Y. Cho and A. Ivanisevic, *Langmuir*, 2006, **22**, 8670–8674.
- 106 Y. Cho and A. Ivanisevic, *J. Phys. Chem. B*, 2004, **108**, 15223–15228.
- 107 T. Vijaykumar, N. S. John and G. U. Kulkarni, *Solid State Sci.*, 2005, **7**, 1475–1478.
- 108 G. Gundiah, N. S. John, P. J. Thomas, G. U. Kulkarni, C. N. R. Rao and S. Heun, *Appl. Phys. Lett.*, 2004, **84**, 5341–5343.
- 109 B. W. Maynor, Y. Li and J. Liu, *Langmuir*, 2001, **17**, 2575–2578.
- 110 L. Basabe-Desmonts, C. C. Wu, K. O. van der Werf, M. Peter, M. Bennink, C. Otto, A. H. Velders, D. N. Reinhoudt, V. Subramaniam and M. Crego-Calama, *ChemPhysChem*, 2008, **9**, 1680–1687.
- 111 R. D. Piner and C. A. Mirkin, *Langmuir*, 1997, **13**, 6864–6868.
- 112 K. B. Lee, S. J. Park, C. A. Mirkin, J. C. Smith and M. Mrksich, *Science*, 2002, **295**, 1702–1705.
- 113 D. J. Pena, M. P. Raphael and J. M. Byers, *Langmuir*, 2003, **19**, 9028–9032.
- 114 D. S. Ginger, H. Zhang and C. A. Mirkin, *Angew. Chem., Int. Ed.*, 2004, **43**, 30–45.
- 115 S. Lenhart, P. Sun, Y. H. Wang, H. Fuchs and C. A. Mirkin, *Small*, 2007, **3**, 71–75.
- 116 S. Xu and G. Y. Liu, *Langmuir*, 1997, **13**, 127–129.
- 117 P. V. Schwartz, *Langmuir*, 2001, **17**, 5971–5977.
- 118 K. Wadu-Mesthrige, N. A. Amro, J. C. Garno, S. Xu and G. Y. Liu, *Biophys. J.*, 2001, **80**, 1891–1899.
- 119 S. Xu, S. Miller, P. E. Laibinis and G. Y. Liu, *Langmuir*, 1999, **15**, 7244–7251.
- 120 J. R. Kenseth, J. A. Harnisch, V. W. Jones and M. D. Porter, *Langmuir*, 2001, **17**, 4105–4112.
- 121 Y. Hu, A. Das, M. H. Hecht and G. Scoles, *Langmuir*, 2005, **21**, 9103–9109.
- 122 M. Z. Liu and G. Y. Liu, *Langmuir*, 2005, **21**, 1972–1978.
- 123 N. A. Amro, S. Xu and G. Y. Liu, *Langmuir*, 2000, **16**, 3006–3009.
- 124 G. Y. Liu and N. A. Amro, *Proc. Natl. Acad. Sci. U. S. A.*, 2002, **99**, 5165–5170.
- 125 M. Z. Liu, N. A. Amro, C. S. Chow and G. Y. Liu, *Nano Lett.*, 2002, **2**, 863–867.
- 126 R. Garcia, R. V. Martinez and J. Martinez, *Chem. Soc. Rev.*, 2006, **35**, 29–38.
- 127 Y. Azechi, K. Takemura, Y. Shinohara, Y. Nishimura and T. Arai, *J. Phys. Org. Chem.*, 2007, **20**, 864–871.
- 128 E. S. Snow and P. M. Campbell, *Science*, 1995, **270**, 1639–1641.
- 129 T. Yoshinobu, J. Suzuki, H. Kurooka, W. C. Moon and H. Iwasaki, *Electrochim. Acta*, 2003, **48**, 3131–3135.
- 130 H. Rauter, V. Matyushin, Y. Alguel, F. Pittner and T. Schalkhammer, *Macromol. Symp.*, 2004, **217**, 109–133.
- 131 A. Maalouf, M. Gadonna and D. Bosc, *J. Phys. D: Appl. Phys.*, 2009, **42**.
- 132 K. S. Song, T. Hiraki, H. Umezawa and H. Kawarada, *Applied Physics Letters*, 2007, **90**.
- 133 S. Britland, E. Perezarnaud, P. Clark, B. McGinn, P. Connolly and G. Moores, *Biotechnol. Prog.*, 1992, **8**, 155–160.

- 134 J. M. Taguenang, A. Kassu and A. Sharma, *J. Colloid Interface Sci.*, 2006, **303**, 525–531.
- 135 B. R. Ringeisen, J. Callahan, P. K. Wu, A. Pique, B. Spargo, R. A. McGill, M. Bucaro, H. Kim, D. M. Bubb and D. B. Chrisey, *Langmuir*, 2001, **17**, 3472–3479.
- 136 A. Gerardino, A. Notargiacomo and P. Morales, *Microelectron. Eng.*, 2003, **67–68**, 923–929.
- 137 P. Serra, J. M. Fernandez-Pradas, F. X. Berthet, M. Colina, J. Elvira and J. L. Morenza, *Applied Physics a-Materials Science & Processing*, 2004, **79**, 949–952.
- 138 M. Colina, P. Serra, J. M. Fernández-Pradas, L. Sevilla and J. L. Morenza, *Biosens. Bioelectron.*, 2005, **20**, 1638–1642.
- 139 B. R. Ringeisen, D. B. Chrisey, A. Piqué, H. D. Young, R. Modi, M. Bucaro, J. Jones-Meehan and B. J. Spargo, *Biomaterials*, 2002, **23**, 161–166.
- 140 D. B. Chrisey, A. Pique, R. A. McGill, J. S. Horwitz, B. R. Ringeisen, D. M. Bubb and P. K. Wu, *Chem. Rev.*, 2003, **103**, 553–576.
- 141 K. L. Christman, V. D. Enriquez-Rios and H. D. Maynard, *Soft Matter*, 2006, **2**, 928–939.
- 142 R. Abargues, J. Marques-Hueso, J. Canet-Ferrer, E. Pedrueza, J. L. Valdes, E. Jimenez and J. P. Martinez-Pastor, *Nanotechnology*, 2008, **19**.
- 143 S. Borini, S. D'Auria, M. Rossi and A. M. Rossi, *Lab Chip*, 2005, **5**, 1048–1052.
- 144 H. P. Brack, C. Padeste, M. Slaski, S. Alkan and H. H. Solak, *J. Am. Chem. Soc.*, 2004, **126**, 1004–1005.
- 145 H. Muguruma and I. Karube, *TrAC, Trends Anal. Chem.*, 1999, **18**, 62–68.
- 146 A. Hiratsuka, K. Kojima, H. Muguruma, K. H. Lee, H. Suzuki and I. Karube, *Biosens. Bioelectron.*, 2005, **21**, 957–964.
- 147 G. Kampfrath and R. Hintsche, *Analytical Letters*, 1989, **22**, 2423–2431.
- 148 K. Yoshimura, T. Kitade, K. Kitamura and K. Hozumi, *Microchem. J.*, 1991, **43**, 133–142.
- 149 K. Yoshimura and K. Hozumi, *Microchem. J.*, 1996, **53**, 404–412.
- 150 H. Muguruma, Y. Kase and H. Uehara, *Anal. Chem.*, 2005, **77**, 6557–6562.
- 151 H. Muguruma, *TrAC, Trends Anal. Chem.*, 2007, **26**, 433–443.
- 152 J. S. Li, H. Wang, T. Deng, Z. Y. Wu, G. L. Shen and R. Q. Yu, *Biosensors & Bioelectronics*, 2004, **20**, 841–847.
- 153 K. Nakanishi, H. Muguruma and I. Karube, *Anal. Chem.*, 1996, **68**, 1695–1700.
- 154 S. Kurosawa, T. Hirokawa, K. Kashima, H. Aizawa, J. W. Park, M. Tozuka, Y. Yoshimi and K. Hirano, *J. Photopolym. Sci. Technol.*, 2002, **15**, 323–329.
- 155 H. Wang, C. C. Wang, C. X. Lei, Z. Y. Wu, G. L. Shen and R. Q. Yu, *Anal. Bioanal. Chem.*, 2003, **377**, 632–638.
- 156 H. Muguruma, R. Nagata, R. Nakamura, K. Sato, S. Uchiyama and I. Karube, *Anal. Sci.*, 2000, **16**, 347–348.
- 157 M. Duman, R. Saber and E. Piskin, *Biosens. Bioelectron.*, 2003, **18**, 1355–1363.
- 158 Z. H. Zhang, Q. Chen, W. Knoll, R. Foerch, R. Holcomb and D. Roitman, *Macromolecules*, 2003, **36**, 7689–7694.